Zoologica Scripta

New chiropterans from the middle Eocene of Shanghuang (Jiangsu Province, Coastal China): new insight into the dawn horseshoe bats (Rhinolophidae) in Asia

Anthony Ravel, Laurent Marivaux, Tao Qi, Yuan-Qing Wang & K. Christopher Beard

Submitted: 26 March 2013
Accepted: 6 June 2013
doi:10.1111/zsc.12027

Ravel, A., Marivaux, L., Qi, T., Wang, Y.-Q., Beard, K. C. (2014). New chiropterans from the middle Eocene of Shanghuang (Jiangsu Province, Coastal China): new insight into the dawn horseshoe bats (Rhinolophidae) in Asia —*Zoologica Scripta*, *43*, 1–23.

Until recently, the fossil record of Paleogene bats in Asia primarily included extinct families (i.e. 'Eochiroptera') from the early Eocene of Vastan in India and from the middle-late Eocene of the Liguanqiao and Yuanqu basins in central China. Here, we describe a new fauna of Chiroptera from the middle Eocene Shanghuang fissure fillings of China. The fauna includes abundant material referred to a new rhinolophid (*Protorhinolophus shanghuangensis* gen. and sp. n.), one specimen of a possible rhinopomatid and several indeterminate rhinolophoids. This new bat assemblage constitutes the earliest record of extant families of microbats in Asia. Because it lacks representatives of 'Eochiroptera', this Shanghuang bat fauna indicates significant turnover in Asian bat communities. The dental pattern of *P. shanghuangensis* shows a mosaic of primitive and derived features ('Eochiroptera' *vs* Rhinolophidae dental characteristics), suggesting that this taxon occupies a basal position among the Rhinolophidae. Rhinolophids were already well diversified at the end of the late Eocene in Europe. Interestingly, many dental characteristics of *Protorhinolophus* are also found in a primitive rhinolophoid taxon, *Vaylatsia*, from the middle Eocene to late Oligocene of Europe, supporting a close relationship between these taxa. These affinities testify to the widespread Eurasian distribution of rhinolophoids during the Eocene and are consistent with a westward dispersal of the group from eastern Asia to Europe owing to the greater antiquity of *Protorhinolophus*.

Corresponding author: *Anthony Ravel, Institut des Sciences de l'Evolution (ISEM, UMR 5554 CNRS/UM2/IRD), Université Montpellier II, Place E. Bataillon – CC 064, 34095 Montpellier Cedex 5, France. E-mail: anthony.ravel@univ-montp2.fr*

Anthony Ravel, and Laurent Marivaux, Institut des Sciences de l'Evolution (ISEM, UMR 5554 CNRS/UM2/IRD), Université Montpellier II, Place E. Bataillon – CC 064, 34095, Montpellier Cedex 5, France. E-mails: anthony.ravel@univ-montp2.fr, laurent.marivaux@univ-montp2.fr

Tao Qi, and Yuan-Qing Wang, Institute of Vertebrate Paleontology and Paleoanthropology, Chinese Academy of Sciences, 142 Xi Zhi Men Wai Street, Beijing, 100044, China, wangyuanqing@ivpp.ac.cn

Kenneth Christopher Beard, Section of Vertebrate Paleontology, Carnegie Museum of Natural History, 4400 Forbes Avenue, Pittsburgh, PA, 15213, USA. E-mail: beardc@carnegiemnh.org

Introduction

The Paleogene fossil record of Chiroptera is poorly documented in Asia compared with those of Europe, North America or even Africa (Gunnell & Simmons 2005; Eiting & Gunnell 2009). In Asia, only a few localities have been discovered so far. The oldest Asian bat fauna derives from the Vastan lignite mine located in Gujarat in western India, which dates to the early Eocene (Rana *et al.* 2005; Smith *et al.* 2007). Although this locality has yielded abundant fossil elements of bats documenting upper and lower dentitions, only lower jaws have been described so far. These fossils document seven new species, including one icaronycterid (*Icaronycteris sigei*), two archaeonycterids (*Protonycteris gunnelli*, *Archaeonycteris storchi*), two hassianycterids (*Hassianycteris kumari*, *Cambaya complexus*), one palaeochiropterygid (*Microchiropteryx folieae*) and *Jaegeria cambayensis*

of indeterminate family status (Smith *et al.* 2007). Most of these Vastan bats are documented as 'Eochiroptera', a name commonly used to designate a paraphyletic group that includes all extinct stem-chiropterans branching successively at the base of the bat phylogeny (Simmons & Geisler 1998; Simmons 2005). The exception is *J. cambayensis*, which could belong to Palaeochiropterygidae or a modern family (Smith *et al.* 2007). This Indian bat assemblage resembles certain Eocene European microchiropteran faunas, especially those from the early Eocene of the Paris Basin (Russell *et al.* 1973) and the early middle Eocene of Messel in Germany (Habersetzer & Storch 1987), which primarily document 'Eochiroptera'. In central China, bats occur in the middle-late Eocene deposits of the Liguanqiao Basin (Henan Province) and Yuanqu Basin (Shanxi Province). These Chinese fossils document essentially 'Eochiroptera', notably two species of Palaeochiropterygidae (*Lapichiropteryx xiei* and *Lapichiropteryx* sp.) and several indeterminate specimens referred to the Icaronycteridae and Archaeonycteridae (Tong 1997). Microchiropterans have also been reported from the early-middle Eocene Kuldana Formation of Pakistan (Chorlakki; Russell & Gingerich 1981). However, this fossil material is highly fragmentary (only two teeth; M^3 and $M_{1/2}$), and their systematic attribution remains questionable. Of these teeth, the lower molar could be referred to a member of Palaeochiropterygidae, while the upper molar shows an unusual combination of features, which is otherwise unknown in Chiroptera. Interestingly, Asia has also yielded the oldest occurrence of Megachiroptera (Ducrocq *et al.* 1993). The presence of this extant family of bats (i.e. Pteropodidae) in the Paleogene of Asia is based on the discovery of one isolated P_3 from the famous Krabi coal mine of peninsular Thailand, which dates to the latest Eocene.

The locality of Shanghuang consists of five fissure fillings within the Triassic Shangqinglong limestone near Shanghuang village in Liyang County, southern Jiangsu Province, coastal China (Métais *et al.* 2008; Fig. 1). The karstic infillings have produced a high diversity of fossil mammals including primates, rodents, artiodactyls, perissodactyls, marsupials, tillodonts, condylarths, carnivores, creodonts, lagomorphs and eulipotyphlans (Qi *et al.* 1991, 1996; Beard *et al.* 1994; Wang & Dawson 1994; Qi & Beard 1996; Dawson & Wang 2001; Dawson *et al.* 2003; Métais *et al.* 2004, 2005, 2008). Based on mammalian biostratigraphy, fissures A, B and C at Shanghuang are correlated with the Sharamurunian Asian Land Mammal Ages (ALMA; Russell & Zhai 1987) (i.e. late Lutetian–early Bartonian). In contrast, fissures D and E at Shanghuang are considered to be slightly older than the others, being correlated with the Irdinmanhan ALMA (i.e. middle Lutetian). However, the homogeneity of the fauna from all five

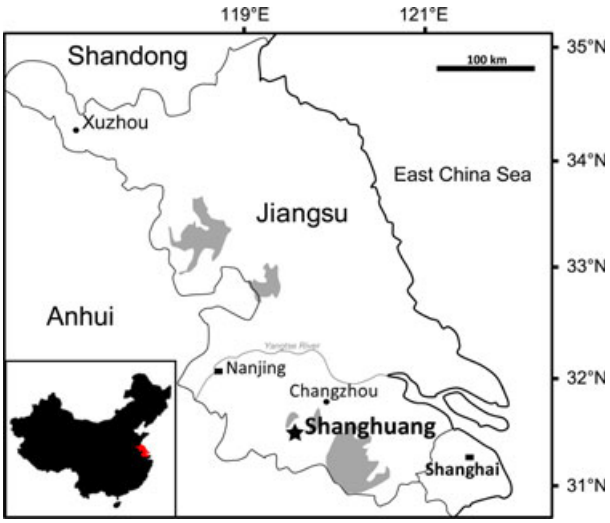

Fig. 1 Localization of the Shanghuang fissure fillings in Jiangsu Province, situated in eastern China (based on Métais *et al.* 2008).

fissures implies a short interval of time in the middle Eocene (Beard *et al.* 1994; Wang & Dawson 1994; Qi & Beard 1996; Qi *et al.* 1996; Métais *et al.* 2008).

Qi *et al.* (1996) identified two species of bats in the Shanghuang fissure fillings, without formally describing any material. Here, we describe dental remains of Chiroptera collected from all of the Shanghuang karstic infillings (A, B, C, D and E). Although most mammalian fossils have been recovered from fissure D (70%; Métais *et al.* 2008), the most abundant and best-preserved bat specimens were collected from fissure A (approximately 50%). The Shanghuang bat fauna is poorly diversified but includes at least four taxa that are well identified and one specimen of an indeterminate microchiropteran family. All of these new taxa are members of the modern groups Rhinolophoidea and Rhinopomatoidea. Given the scarce Paleogene bat fossil record in Asia, these new Shanghuang taxa represent the earliest Asian representatives of these modern families. The dominant species, a new horseshoe bat (Rhinolophidae: *Protorhinolophus shanghuangensis* gen. et sp. n.), is represented by approximately 80% of all known specimens. The specimens are housed in the collections of the Institute of Vertebrate Paleontology and Paleoanthropology (IVPP), Beijing, China. The nomenclature of the dental structures is given on figure 2.

Systematic palaeontology

Order CHIROPTERA Blumenbach, 1779
Suborder MICROCHIROPTERA Dobson, 1875
Superfamily RHINOLOPHOIDEA Bell, 1836 (Weber, 1928)
Family RHINOLOPHIDAE Bell, 1836
Genus Protorhinolophus gen. n
Type species. Protorhinolophus shanghuangensis sp. n.

Diagnosis. As that of the type and only known species.

Etymology. The generic name refers to the antiquity and the primitive morphology of this rhinolophid.

Protorhinolophus shanghuangensis sp. n. (Figs 3–5).

Holotype. **IVPP V18643**, right dentary with P_4-M_3 (Figs 3F and 5B).

Referred specimens. **IVPP V18644.1** (left dentary with alveoli of P_2-M_3; Figs 3G and 5A); **IVPP V18644.9**, **IVPP V18644.8** (Fig. 4J), **IVPP V18644.10** and **IVPP V18648.1** (right C_1); **IVPP V18644.2**, **IVPP V18644.3**, **IVPP V18644.4**, **IVPP V18644.5**, **IVPP V18644.6**, **IVPP V18644.7**, **IVPP V18645.1** and **IVPP V18646.1** (left C_1); **IVPP V18647.1** (right P_2); **IVPP V18647.2**, **IVPP V18646.2** (Fig. 4K) and **IVPP V18644.11** (left P_2; Fig. 4L); **IVPP V18644.13** and **IVPP V18644.14** (right P_4; Fig. 4N); **IVPP V18644.12** (Fig. 4M) and **IVPP V18645.2** (left P_4); **IVPP V18644.15** (right M_1; Fig. 4O); **IVPP V18646.3** (left M_1); **IVPP V18644.34**, **IVPP V18647.3** (Fig. 4P) and **IVPP V18646.4** (left M_2); **IVPP V18644.16**, **IVPP V18645.3** (Fig. 4Q) and **IVPP V18645.4** (left M_3); **IVPP V18644.17** (Fig. 3A), **IVPP V18644.18**, **IVPP V18644.19**, **IVPP V18644.20** and **IVPP V18648.2** (right C^1); **IVPP V18646.5** and **IVPP V18648.3** (left C^1); **IVPP V18647.4** (right P^4); **IVPP V18644.21** (Figs 3B and 4B) and **IVPP V18644.22** (left P^4); **IVPP V18644.25**, **IVPP V18644.26**, **IVPP V18645.5**, **IVPP V18645.6**, **IVPP V18648.4** and **IVPP V18647.5** (right M^1); **IVPP V18644.23** (Figs 3C and 4G), **IVPP V18644.24**, **IVPP V18645.7**, **IVPP V18648.5** and **IVPP V18646.6** (left M^1; Fig. 4C); **IVPP V18644.27** (Fig. 4H), **IVPP V18644.28**, **IVPP V18644.29**, **IVPP V18644.30** (Fig. 4F), **IVPP V18645.9**, **IVPP V18647.6** and **IVPP V18647.7** (right M^2); **IVPP V18644.31** (Fig. 3D), **IVPP V18648.6**, **IVPP V18648.7** (Fig. 4D) and **IVPP V18645.8** (left M^2); **IVPP V18644.33** and **IVPP V18644.34** (right M^3); **IVPP V18644.32** (Fig. 4I) and **IVPP V18645.10** (left M^3; Figs 3E and 4E).

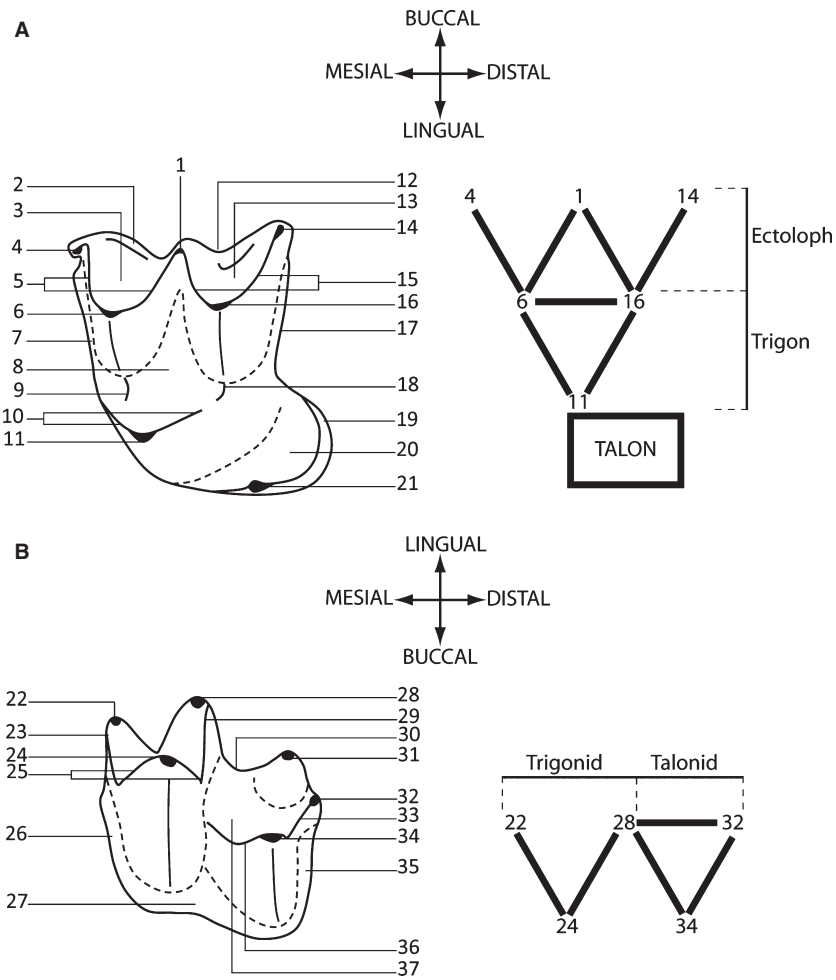

Fig. 2 Occlusal dental morphology of upper and lower molars of chiropterans with related nomenclature, after Van Valen (1966) and Szalay (1969). —A. Upper molar: –1. mesostyle; –2. buccal cingulum; –3. parafossa; –4. parastyle; –5. pre- and postparacrista; –6. paracone; –7. precingulum; –8. protofossa; –9. paraloph; –10. pre- and postprotocrista; –11. protocone; –12. ectoflexus; –13. metafossa; –14. metastyle; –15. pre- and postmetacrista; –16. metacone; –17. postcingulum; –18. metaloph; –19. lingual cingulum; –20. talon basin; –21. hypocone. —B. Lower molar: –22. paraconid; –23. paracristid; –24. protoconid; –25. pre- and postprotoconid; –26. precingulid; –27.buccal cingulid; –28. metaconid; –29. metacristid; –30. entocristid; –31. entoconid; –32. hypoconulid; –33. postcristid; –34. hypoconid; –35. postcingulid; –36. cristid obliqua –37. talonid basin.

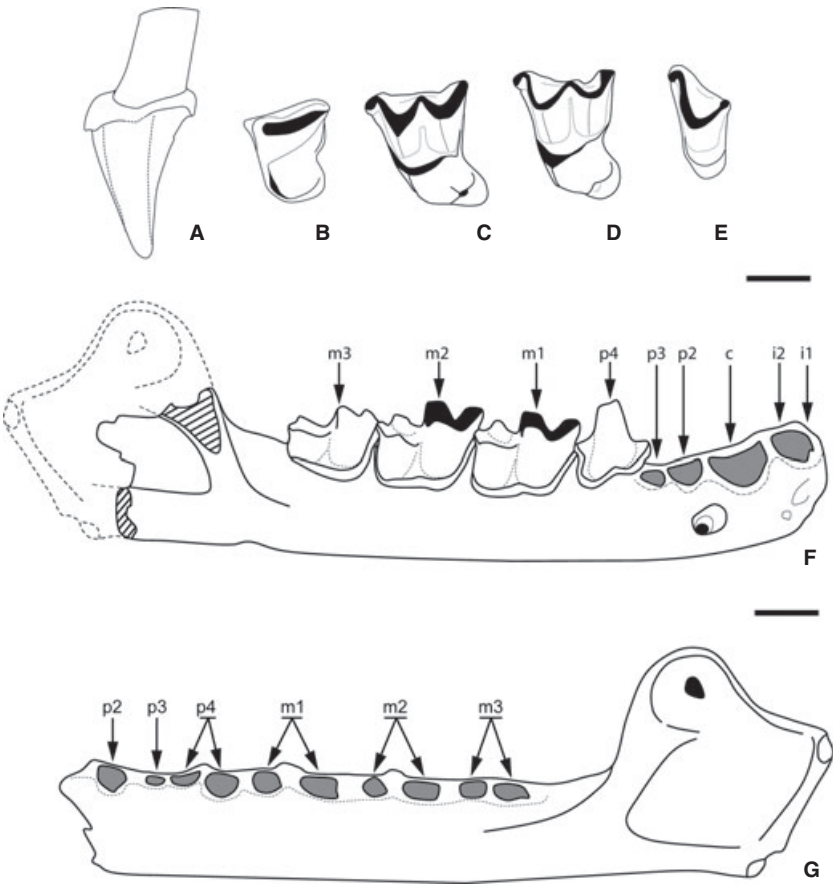

Fig. 3 A–G. Sketches of specimens of *Protorhinolophus shanghuangensis* gen. et sp. n. —A. IVPP V18644.17, right C^1 in buccal view. —B. IVPP V18644.21, left P^4 in occlusal view. —C. IVPP V18644.23, left M^1 in occlusal view. —D. IVPP V18644.31, left M^2 in occlusal view. —E. IVPP V18645.10, left M^3 in occlusal view. The upper canine is a mirror image of the original material. —F. IVPP V18643 (holotype), right mandible with P_4-M_3 in buccal view. —G. IVPP V18644.1, left edentulous mandible in buccal view. The coronoid process and the distal part of the jaw in IVPP V18643 (bold dotted line) is a reconstruction based on the nearly complete edentulous mandible IVPP V18644.1. Scale bar, 1 mm.

Locality and age. (All) Fissure fillings located in the Shanghuang Limestone Quarry, near the village of Shanghuang, Liyang County, southern Jiangsu Province, central coastal China (Fig. 1). The locality is correlated with the Sharamurunian Asian Land Mammal Age (ALMA; Russell & Zhai 1987), middle Eocene.

Etymology. The species name refers to the village of Shanghuang, near the locality.

Diagnosis. Rhinolophidae with an upper canine less curved, P^4 and $M^{1\text{-}2}$ relatively transverse and slightly waisted mesiodistally, $M^{1\text{-}2}$ with a long protofossa closed distally and a strongly projecting talon shelf, small mesostyle on $M^{1\text{-}2}$ displaced lingually with respect to the buccal margin of the crown, a strong lingual cingulum with a trace of hypocone, M^3 small without metacone, metacristae and metastyle, P_3 small and slightly offset buccally with respect to the main mesiodistal axis of the toothrow, P_4 elongated with no paraconid but a long anterior flat plate, and a metaconid well-inferior and twinned to the protoconid, lower molars nyctalodont with a hypoconulid more buccal than the entoconid.

Description. This taxon includes most of the specimens, whose size is considered as average. Measures of the specimens are presented Appendix 1.

The holotype (IVPP V18643: Fig. 3F and 5B) is a nearly complete right dentary bearing P_4-M_3 and the alveoli of I_1, I_2, C_1, P_2 and P_3. The horizontal ramus is thin and straight with two mental foramina: 1 min and situated below $I_{1\text{-}2}$, the other one relatively larger and located between C_1 and P_2. The toothless mandible **IVPP V18644.1** (Figs 3G and 5A) is similar in size and shows the same proportions along the toothrow as in the holotype, allowing it to be attributed to the same species. The coronoid process of **IVPP V18644.1** is low and leans slightly posteriorly. Buccally, the ventral aspect of the dentary shows a well-defined masseteric fossa, which is deep and relatively long.

The crown of the lower canine is sub-triangular in occlusal view with two lobes mesiolingual and distolingual. The main cusp is relatively high compared to the cheek teeth and slightly curved distolingually. The distolingual concave surface of this cusp extends to a wide but short distal basin. The crown has a complete cingulid that produces a minute cuspule at its distolingual extremity. A short

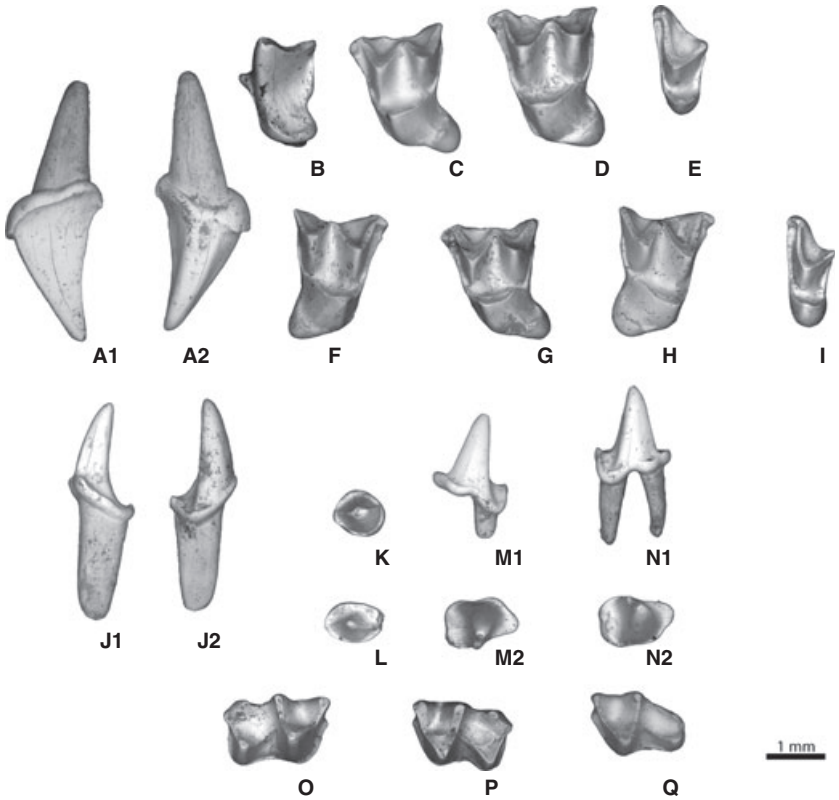

Fig. 4 A–Q. *Protorhinolophus shanghuangensis* from fissures A, B, C, D and E of the middle Eocene of Shanghuang, China. —A. IVPP V18644.17, right C^1 in lingual (A1) and buccal views (A2). —B. IVPP V18644.21, left P^4 in occlusal view. —C. IVPP V18646.6, left M^1 in occlusal view. —D. IVPP V18648.7, left M^2 in occlusal view. —E. IVPP V18645.10, left M^3 in occlusal view. —F. IVPP V18644.30, right M^2 in occlusal view. —G. IVPP V18644.23, left M^1 in occlusal view. —H. IVPP V18644.27, right M^2 in occlusal view. —I. IVPP V18644.32, left M^3 in occlusal view. —J. IVPP V18644.8, right C_1 in lingual (J1) and buccal (J2) views. —K. IVPP V18646.2, left P_2 in occlusal view. —L. IVPP V18644.11, left P_2 in occlusal view. —M. IVPP V18644.12, left P_4 in buccal (M1) and occlusal (M2) views. —N. IVPP V18644.14, right P_4 in buccal (N1) and occlusal (N2) views. —O. IVPP V18644.15, right M_1 in occlusal view. – P. IVPP V18647.3, left M_2 in occlusal view. —Q. IVPP V18645.3, left M_3 in occlusal view. Scale bar, 1 mm.

but high crest extends from the inner surface of the main cusp and joins this distal cuspule.

The second and third lower premolars (P_{2-3}) are not preserved in the holotype (Figs 3F and 5B). However, the alveoli for these teeth indicate that both premolars were single rooted. The alveolus of P_3 is particularly reduced compared with that of P_2, thereby indicating that P_3 was relatively small. Interestingly, the alveolus of P_3 is slightly offset buccally with respect to the main mesiodistal axis of the toothrow. This could indicate that this minute tooth was not highly functional. Given their size (Appendix 1), **IVPP V18644.11**, **IVPP V18647.2**, **IVPP V18647.1** and

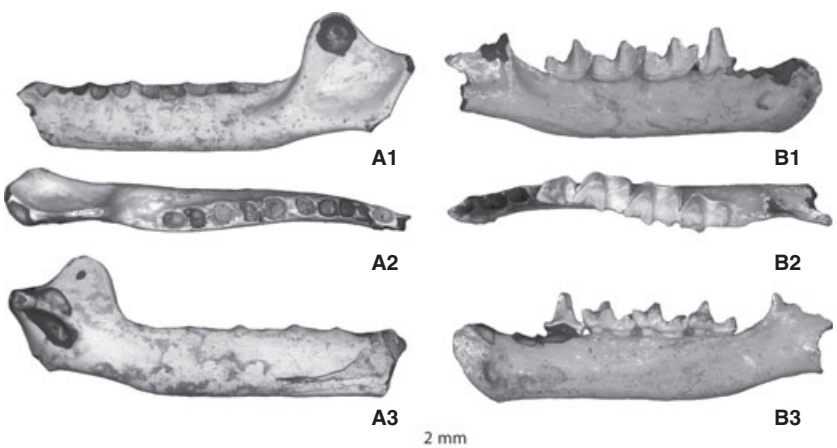

Fig. 5 —A,B. *Protorhinolophus shanghuangensis* from fissures A, B, C, D and E of the middle Eocene of Shanghuang, China. —A. IVPP V18644.1, left edentulous mandible in buccal (A1), occlusal (A2) and lingual (A3) views. —B. IVPP V18643 (Holotype), right mandible with P_4-M_3 in buccal (B1), occlusal (B2) and lingual (B3) views. Scale bar, 1 mm.

IVPP V18646.2 (Figs 4K,L) are identified as P_2 rather than P_3. **IVPP V18644.11** and **IVPP V18646.2** are very small teeth that consist of a single oval tubercle with two cutting edges, which extend from the tip of this tubercle to the mesial and distal margins of the tooth. The crowns of **IVPP V18647.1** and **IVPP V18647.2** are quite different, being very simple in shape, showing a single conical tubercle encircled by a continuous and thin cingulid.

P_4 is doubled-rooted and somewhat offset lingually with respect to the three molars, which are perfectly aligned mesiodistally. In occlusal view, this tooth has a rectangular outline and may appear as premolariform. The protoconid is prominent and conical, forming the main cuspid of the tooth. The metaconid is distal to the protoconid and well inferior to it, with an apex situated midway along the height of the trigonid. There is no distinct paraconid, but a low and long paracristid extends mesiolingually from the protoconid, thereby forming a low mesial plate. The talonid is particularly reduced mesiodistally (virtually absent) and bears a tiny cuspid that could be a minute hypoconid. A longitudinal cristid (?cristid obliqua) extends from this small cuspid to the distal side of the protoconid. The buccal cingulid is thin and continuous.

The lower molars are clearly larger than P_4. M_1 and M_2 are nearly identical in size and morphology, except for the position of the paraconid, which is slightly more mesially projected in M_1. In occlusal view, the outline of the molar crown is rectangular. On $M_{1\text{-}2}$, the trigonid is slightly higher and longer than the talonid, but both are similar in breadth. On all three molars, the trigonid is V-shaped and open lingually. The paraconid appears slightly smaller and more buccal than the metaconid. The protoconid is prominent and dominates both the metaconid and paraconid. The buccal cingulid is continuous and joins the strong pre- and postcingulids. The hypoconid is the most important cuspid of the talonid, but it remains smaller than the trigonid cuspids. The entoconid is reduced and buccally opposed to the hypoconid. Distally, the postcristid extends from the hypoconid to a well-defined hypoconulid, which is well separated and offset distobuccally with respect to the entoconid. The cristid obliqua is long and high and joins the distal wall of the trigonid near its midline. Compared to $M_{1\text{-}2}$, the trigonid of M_3 appears only slightly reduced, while the talonid is strongly reduced, being shorter and compressed buccolingually. The main three cuspids of the talonid are well individualized but very small.

The upper dentition is documented exclusively by isolated teeth. The upper canine is taller and larger than the lower canine. This tooth is robust and conical with a main cusp that is curved slightly backward and which bears two crests. One crest is well marked and extends distally from the tip of the cusp, while the second is weaker and extends mesially. These two crests form the boundaries of the buccal and lingual surfaces of the crown. Mesially, the buccal margin of the canine is bent and is opposed to the concave lingual surface. The cingulum is continuous around the cusp, but it appears more massive and higher at the base of the mesial aspect of the cusp. A minute tubercle on the most distal part of the tooth marks the junction between the distal crest and the cingulum.

P^4 is triple-rooted with two buccal roots and one lingual root. The crown is slightly waisted mesiodistally. The paracone is the only cusp of the crown and it occupies a mesiobuccal position. This cusp is salient and bears a very high shearing crest, which runs from the apex of the cusp to the distobuccal margin of the crown. The paracone and its postparacrista form a high and trenchant (blade-like) buccal margin, the lingual surface of which extends lingually to form a very broad basin. A prominent lingual cingulum surrounds the talon basin and forms a small tubercle mesiolingually.

M^1 and M^2 are roughly equal in size and show a rectangular outline, with a buccolingual (i.e. transverse) long axis. M^1 differs from M^2 in having less transverse proportions, but both teeth show a very similar occlusal pattern. Their crowns are slightly waisted mesiodistally and their buccal margin is wider than the lingual part of the trigon basin. In both teeth, the dilambdodont W-shaped ectoloph is particularly well developed. It appears somewhat asymmetrical due to the position of the metacone, which is slightly more buccal than the paracone. The inflected parastylar shelf is more complex than the metastylar shelf. The ectoflexus is deeper on M^2 than on M^1, in which the buccal side is nearly linear. The ectoflexus on M^1 owes to the position of the metastyle, which projects farther buccally than the parastyle. On M^2, there is a notch between the parastyle and the precingulum for the junction with the metastyle of M^1. On both teeth, the mesostyle is well developed but is set back from the buccal margin of the crown. The pre- and postprotocristae close the protofossa and join the pre- and postcingulum, respectively. On most specimens, there is neither loph nor conule. However, some upper molars show a metaloph with a trace of metaconule (IVPP V18648.7; Fig. 4D) or a paraloph with a trace of paraconule (IVPP V18644.30; Fig. 4F), or both (IVPP V18644.23 and IVPP V18646.6; Fig. 4C). The short paraloph joins both the preprotocrista and precingulum, while the metaloph joins both the postprocrista and postcingulum. The protocone is larger but more salient than the two buccal cusps. It is canted mesially and nearly opposed to the paracone. The lingual surface of the protocone extends distolingually to make a talon. The lingual cingulum is not continuous and appears interrupted on the mesiolingual face of the protocone. Distally, it forms a thickened lobe

on the distolingual margin of the crown with a trace of hypocone. It is developed at the distolingual base of the protocone, but remains very short and thin. The third upper molars are half the size of M^{1-2}. M^3 also differs from the other molars in lacking the metacone, metacrista, metastyle, and the lingual cingulum. There is a small mesostyle distolingual to the paracone, at the distal extremity of a short postparacrista. The preparacrista is well developed and extends buccally to join a parastylar shelf. The protocone is small and appears as a rounded enamel swelling lingual to the paracone. There is no lingual cingulum.

Comparison. The comparison between *P. shanghuangensis* and the paleochiropterigyd *L. xiei* is relevant because these two Chinese taxa are roughly the same age (Tong 1997). *Lapichiropteryx xiei* was found in the Zhaili Member of the Heti Formation, Yuanqu County of Shanxi Province in central China (approximately 800 km north-west of Shanghuang). This locality is late middle Eocene in age (i.e. Sharamurunian ALMA) (Berggren & Prothero 1992; Tong *et al.* 1995; Beard *et al.* 1996; Guo *et al.* 2000), and as such is slightly younger than the Shanghuang fissure fillings. *L. xiei* differs from *P. shanghuangensis* in having a mandible with a curved ramus, a short diastema between the premolars and the presence of a double-rooted P_3 (seemingly more functional than that of *P. shanghuangensis*), and in the unreduced size of its M_3, which is similar to that of M_{1-2}. In contrast to *Lapichiropteryx*, the lower molars of *P. shanghuangensis* have a relatively longer trigonid and the hypoconid is thinner and less buccally displaced. In addition, on the upper molars, the new Chinese bat is characterized by a deeper ectoflexus, a more opened ectoloph, a stronger and more projecting distolingual lobe, a discontinuous lingual cingulum, and by the absence of metacone and smaller protocone on M^3. The P^4 of *P. shanghuangensis* is more transversely developed and shows an extensive talon basin.

The bat fauna from Vastan in India testifies to the diversity of stem chiropterans ('Eochiroptera') in South Asia during the early Eocene (Smith *et al.* 2007). The Shanghuang bat differs substantially from *Icaronycteris sigei*, *P. gunnelli*, *A. storchi*, *C. complexus* and *J. cambayensis* in having a reduced and single-rooted P_3, a mandible with a small coronoid process leaning backward, and a thin ramus that is curved mesiolingually. The P_4 of *P. shanghuangensis* has no paraconid, the talonid is sharply reduced and the metaconid is partially fused with the protoconid, a condition which contrasts with the more nearly molariform P_4 observed in *I. sigei*, *P. gunnelli* and *A. storchi*. This tooth is more similar to that of *H. kumari*, *C. complexus* and *J. cambayensis*, which show a more advanced P_4 structure than in the Icaronycteridae and Archaeonycteridae. The lower molars of *P. shanghuangensis* also differ from all Vastan bats in having more open trigonids with paraconids that project mesially and in showing no significant difference in elevation between trigonid and talonid. The position of the hypoconulid on the first and second lower molars of *P. shanghuangensis* is, however, similar to that seen on lower molars of 'Eochiroptera' (Simmons & Geisler 1998; Smith *et al.* 2007). The upper molars of the Indian bats have not yet been described, precluding any direct comparisons. However, the upper dentition of *Protorhinolophus* resembles the upper dentition of Eocene European 'Eochiroptera' from the Paris Basin and Messel (Icaronycteridae, Archaeonycteridae and Palaeochiropterygidae; Russell & Sigé 1970; Russell *et al.* 1973), notably in the transverse development of the first and second upper molars, the occlusal outlines of these teeth, which are waisted mesiodistally, the broad distolingual lobe and the closure of the protofossa in the trigon. Some teeth of *P. shanghuangensis* display traces of paraconule and/or metaconule, which are connected to the paraloph and metaloph, respectively (**IVPP V18644.24, IVPP V18644.25**, **IVPP V18648.5** and **IVPP V18646.6**). The presence of both the paraconule and metaconule is characteristic of the Eocene Chiroptera from Europe (Russell & Sigé 1970; Russell *et al.* 1973). In contrast, the upper molars of *P. shanghuangensis* differ from these archaic bats in showing a very open ectoloph, a shallower ectoflexus, a well-developed and salient mesostyle, the virtual absence of loph and conule, a slender protocone, a discontinuous lingual cingulum and stronger distal projection of the lingual lobe. The M^3 of *P. shanghuangensis* has a very simple structure, which is characterized by the absence of metacone, metacristae, metastyle and lingual cingulum. Furthermore, this tooth is reduced in breadth compared to M^2. The morphology and relative size of the M^3 in *P. shanghuangensis* is clearly distinct from the primitive condition characterizing the M^3 observed in all 'Eochiroptera' (Smith *et al.* 2012). In the latter taxa, the M^3 shows a well-developed metacone, has a premetacrista and develops a small lingual cingulum.

Chiroptera from the early-middle Eocene of the Kuldana Formation (Kohat) of Pakistan are known only by one M^3 and a fragment of a lower molar (Russell & Gingerich 1981). The M^3 of *P. shanghuangensis* differs from the Pakistani specimen in lacking the metacone and premetacrista. As in lower molars of *Protorhinolophus*, the talonid of the lower molar from Pakistan displays a nyctalodont structure, but the position of the hypoconulid is not specified, which limits the comparisons.

Extant families of microbats are unknown in Asia until the Pleistocene (Simmons 2005; Eiting & Gunnell 2009). However, *Protorhinolophus* shows many dental characteristics of Rhinolophoidea. A slender ramus with a low coronoid process of the mandible, a reduced P_3, lower molars

with an open trigonid, their talonid as wide as their trigonid and the nyctalodont structure of the talonid are all typical rhinolophoid features (e.g. Sigé 1978, 1991; Sevilla 1990). In the upper dentition, *Protorhinolophus* shares with the Rhinolophoidea the presence of a transverse P^4, an open W-shaped ectoloph on $M^{1\text{-}2}$, the paracone and metacone near the buccal margin of the crown, the development of a talon and a slender protocone.

Rhinolophoids include several modern bat families such as Hipposideridae, Rhinolophidae, Megadermatidae and Nycteridae (Simmons & Geisler 1998; Simmons & Conway 2003; Simmons 2005). It is generally admitted that the Megadermatidae represent the sister group of the Hipposideridae-Rhinolophidae clade (Simmons & Geisler 1998; Springer *et al.* 2001; Gunnell & Simmons 2005). The morphology of the upper molars of *Protorhinolophus* differs from those of Megadermatidae (*Megaderma*, *Macroderma*, *Lavia* and *Cardioderma*) in several details. Indeed, megadermatids have upper molars showing a 'distorted' W-shaped ectoloph, which includes a long postmetacrista that projects distobuccally, and a very short protocone that overhangs the talon basin, which is very extensive distolingually. Furthermore, the upper canines of Megadermatidae display a large secondary cusp that contrasts with the simple morphology of the upper canines of *Protorhinolophus*. The phylogenetic position of the Nycteridae with respect to the Rhinolophoidea remains in a state of flux. Some molecular phylogenies have excluded the Nycteridae from the Rhinolophoidea (Eick *et al.* 2005; Simmons 2005; Teeling *et al.* 2005). *Protorhinolophus* differs from the Nycteridae (i.e. *Nycteris*) in having a large P_4, a small P_3, lower molars with the entoconid well developed and distal in position with respect to the hypoconid, the hypoconulid displaced buccally and upper molars ($M^{1\text{-}2}$) showing a shallower and single ectoflexus, an open protofossa, a larger protocone and broad lingual cingulum with a trace of hypocone.

Living Hipposideridae and Rhinolophidae are very similar in terms of dental morphology. From the small size of the P_3 alveolus observable on the holotype and **IVPP V18644.1**, it can be expected that the P_3 of *Protorhinolophus* was very small and perhaps not highly functional. In the Rhinolophidae, the P_3 is vestigial (very reduced), while in Hipposideridae, the P_3 is lost. *Protorhinolophus* displays a suite of dental traits, including the presence of an external cingulum on the upper canine, the junction between the long postprotocrista and the postcingulum on upper molars, the well-developed distolingual shelf and the transverse development of the P^4, which are more characteristic of rhinolophids than hipposiderids. However, the small size and the reduction in the distal part of M^3 in *Protorhinolophus* resemble conditions found in hipposiderids. This is correlated with the reduction in the talonid of M_3 in the holotype of *P. shanghuangensis*, a condition also observed in M_3 of *Hipposideros*, *Asellia* and *Anthops*. *Protorhinolophus* also resembles Hipposideridae in having upper molars with a broad lingual cingulum and moderate development of the talon basin, which is more extensive in upper teeth of rhinolophids.

The Rhinolophidae are a monotypic family. The only genus, *Rhinolophus*, is recorded in the late Eocene and early Oligocene of the Quercy (Sigé 1978) and the late Oligocene of Carrascosa del Campo (central Spain; Sevilla 1990). Basically, *Protorhinolophus* exhibits a more primitive dental pattern than *Rhinolophus*: the P_3 in the holotype is relatively more developed, the P_4 bears a small metaconid, the upper canine is less curved and $M^{1\text{-}2}$ are more transversely developed and waisted mesiodistally, with a small mesostyle set in from the buccal edge of the crown and with a broad lingual lobe bearing a hypocone shelf. Some upper molars of *Protorhinolophus* retained both the paraloph and metaloph, which bear minute paraconule and metaconule, respectively. The presence of these structures on the upper molars of *Protorhinolophus* and *Vaylatsia*, and their absence on *Rhinolophus* and the other Hipposideridae would suggest a reversion of these characters in these formers. Contrary to the Rhinolophidae, the Hipposideridae are well diversified in Europe, Africa and Arabia since the middle Eocene. Hipposiderids from the middle Eocene to late Oligocene karstic infillings of the Quercy (France) include three genera: *Hipposideros* (*Pseudorhinolophus*), *Palaeophyllophora* and *Vaylatsia* (Sigé 1978, 1990, 1997; Sigé & Legendre 1983). *Hipposideros* (*Brachipposideros*) is also documented in the early Oligocene of Taqah in the Sultanate of Oman (Sigé *et al.* 1994). Like *Protorhinolophus* and *Rhinolophus*, *Palaeophyllophora* and *Vaylatsia* retain P_3, their P_4 displays a metaconid, which is partially merged with the protoconid, and the $M_{1\text{-}2}$ show their hypoconulid located far distobuccally from the entoconid. However, the lower dentition of *Protorhinolophus* differs from *Palaeophyllophora* in having a larger P_3, a more elongated P_4 and $M_{1\text{-}2}$ showing a longer talonid. In addition, the upper molars of *Palaeophyllophora* have an unusual morphology, which differs substantially from that of *Protorhinolophus*. This is particularly shown in the structure of the ectoloph, which displays a small mesostyle that occupies a very buccal position and is connected to a very short centrocristae, and the inner surface of the paracone and metacone, which appears in continuity with the buccal extension of the protofossa. In contrast, the dental morphology of *Vaylatsia* is reminiscent of that of *Protorhinolophus*. The main distinctions are observed on the upper molars: the $M^{1\text{-}2}$ of *Protorhinolophus* differ from those of *Vaylatsia* in being more transversely developed, in having a smaller mesostyle retracted from the buccal margin and

a stronger talon with a robust cingulum that bears a trace of hypocone, and in the absence of both metacone and metacristae on the very small M^3. The distal edge of the upper canines of *Vaylatsia* are also strongly curved, a condition which clearly contrasts with the less curved cusp of the canine of *Protorhinolophus*.

Family ?RHINOLOPHIDAE Bell, 1836

Gen. and sp. indet. (Fig. 6).

Referred specimens. **IVPP V18649.1** (right M^2; Fig. 6C); **IVPP V18649.2** (left M^2; Fig. 6D); **IVPP V18649.3** (left M^3; Fig. 6E).

Locality and age. Fissure filling B located in the Shanghuang Limestone Quarry, near the village of Shanghuang, Liyang County, southern Jiangsu Province, central coastal China. The locality is correlated with the Sharamurunian Asian Land Mammal Age (ALMA; Russell & Zhai 1987), middle Eocene.

Description. These small upper molars [**IVPP V18649.1** (1.40 × 1.75) and **IVPP V18649.2** (1.46 × 1.79); Appendix 1] are wider than long (i.e. transverse) and exhibit short talons that are consistent with their identification as M^2. The crown of these molars is waisted distally. The ectoloph is open but compressed distally. The pre- and postparacristae form a more open V-shape than do the pre- and postmetacristae. The parastyle is hook-like and projects mesially (more on **IVPP V18649.2** than on **IVPP V18649.1**; Figs 6C,D). The position of the parastylar shelf is as buccal as the metastylar shelf, which is straight. The mesostyle is less buccal in position than the other two styles and does not exceed the labial margin of the crown. The precingulum is longer and wider than the postcingulum. The protocone is compressed buccolingually. The lingual cusp is mesially canted but remains slightly more distal than the paracone. The pre- and postcingula join pre- and postprotocristae, respectively, closing the protofossa bilaterally. A thin lingual cingulum surrounds the distal base of the protocone, thereby forming a very short talon. The size and morphology of **IVPP V18649.3** (Fig. 6E) correspond with that of the other isolated upper molars referred to this taxon. This M^3 differs from the more mesial upper molar loci referred to this taxon in lacking metacone and metastyle. The mesostyle is well developed buccally, which involves a flexion on the buccal edge. A short crest extends distolingually from the mesostyle, making a distal lobe of the crown. The extensive protofossa is open distally. The small protocone constitutes the principal structure on the lingual side of the tooth. There is no lingual cingulum.

Comparison. These specimens are significantly smaller than *P. shanghuangensis* but more nearly similar in size to

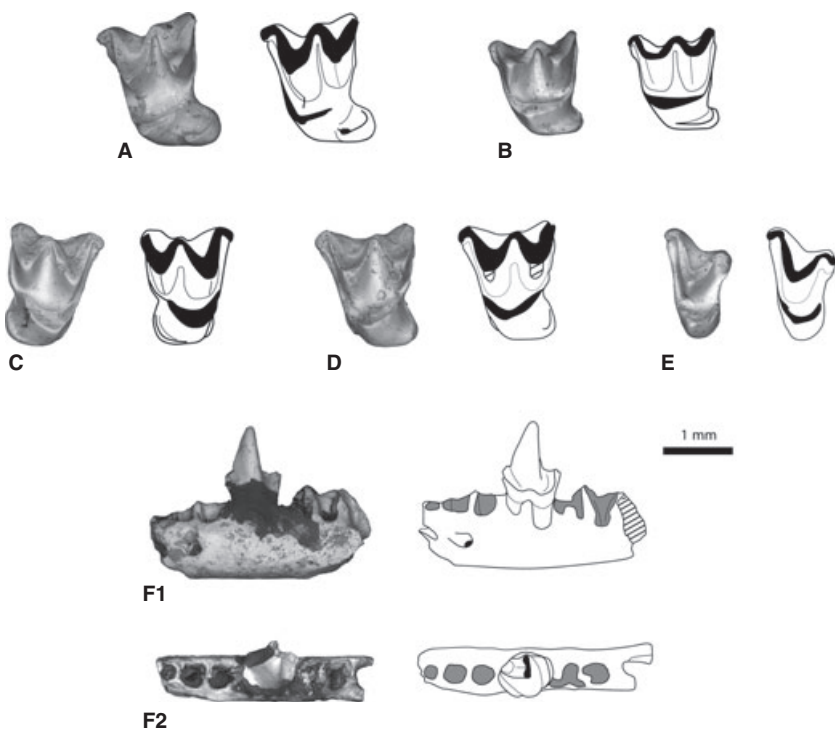

Fig. 6 A. Rhinopomatidae gen. et sp. indet., IVPP V18651, left M^2 in occlusal view —B. Rhinolophoidea, family, gen. et sp. indet., IVPP V18650, left $M^{1/2}$ in occlusal view —C–E. ? Rhinolophidae gen. et sp. indet. —C. IVPP V18649.1, right M^2 in occlusal view. —D. IVPP V18649.2, left M^2 in occlusal view. —E. IVPP V18649.3, left M^3 in occlusal view —F. Microchiroptera indet., IVPP V18652, left dentary fragment with P_4 in buccal view (F1) and occlusal (F2) views. SEM pictures are at left and sketches of specimens at right. Scale bar, 1 mm.

IVPP V18650 from fissure C. Like *Protorhinolophus*, the two teeth from fissure B have rhinolophoid affinities, as shown by the ectoloph being open buccally, the presence of a slender protocone and the development of a talon. **IVPP V18649.1** and **IVPP V18649.2** are buccolingually broad like the upper molars of *Protorhinolophus*. They also share the junction of the pre- and postprotocristae with the pre- and postcingula, respectively. The small projection of the talon is rhinolophid-like. The M^3 of this taxon differs from those of *Protorhinolophus* in having a very short premetacrista that extends distally from a well-developed mesostyle. As mentioned earlier, the dental distinctions between Hipposideridae and Rhinolophidae are tenuous, especially for primitive taxa. However, some features depicted on these two M^2 and the M^3 from fissure B more closely approximate the dental pattern of extant Rhinolophidae. The precise systematic attribution of these fossils requires further morphological support than current data allow.

Superfamily RHINOLOPHOIDEA Bell, 1836 (Weber, 1928)

Fam., gen. et sp. indet. (Fig. 6).

Referred specimen. **IVPP V18650** (left $M^{1\text{-}2}$; Fig. 6B), only known specimen.

Locality and age. Fissure filling C located in the Shanghuang Limestone Quarry, near the village of Shanghuang, Liyang County, southern Jiangsu Province, central coastal China. The locality is correlated with the Sharamurunian Asian Land Mammal Age (ALMA), middle Eocene.

Description. This nearly square upper molar is relatively small (1.3 × 1.45; Appendix 1) compared to the other bat specimens from Shanghuang. The dilambdodont ectoloph is well opened and constitutes the main part of the tooth. It is also strongly invaginated due to a deep, double ectoflexus. The mesostylar shelf is narrow and curved, and distal to the parastyle. This latter structure makes a small mesial bend. In contrast, the metastyle is straight and more buccally displaced than the mesostyle and parastyle. The paracone and metacone are broadly separated by a long protofossa, which extends to the mesostylar shelf. The paracone is slightly more lingual than the metacone, but both have the same size. The pre- and postprotocristae join the thin pre- and postcingula, which both enclose and isolate a very deep and broad protofossa. The protocone is canted mesially and very lingual in position. This cusp is compressed buccolingually and less voluminous than the paracone and metacone. The distal surface of the protocone extends to a short talon that extends distally but not lingually. The talon basin is bounded distally by a moderately developed distolingual cingulum.

Comparison. This tooth represents a smaller species than *P. shanghuangensis*. Despite this clear difference in size, **IVPP V18650** displays the same rhinolophoid characteristics found in *Protorhinolophus*. This is particularly shown by the development of the talon, the buccolingually compressed protocone and the presence of a broadly open ectoloph. Although the connections of the pre- and postprotocristae with the pre- and postcingula, respectively, are found in upper molars of *Protorhinolophus*, this pattern also occurs in certain extinct Hipposideridae (*Vaylatsia*), extant Rhinolophidae (*Rhinolophus*) and archaic bats (i.e. 'Eochiroptera') (Smith *et al.* 2012). Despite this primitive arrangement, the overall morphology of **IVPP V18650** appears somewhat more evolutionarily advanced than that characterizing 'Eochiroptera' and some extant Rhinolophoidea. In occlusal view, the square outline of the crown of **IVPP V18650** is similar to that seen on upper molars of some species of Hipposideridae and Nycteridae, notably *Triaenops furculus*, *Aselliscus wheeleri* and *Nycteris nana*. The occlusal outline of this upper molar is linked to the long and wide protofossa that extends to the buccal margin of the crown, between the paracone and metacone, which are widely spaced. The moderate extension of the talon basin is more hipposiderid-like than nycteridlike. However, the precise systematic attribution of this specimen remains unclear given the very limited documentation of this species, which will require further morphological support than current data allow.

Superfamily? RHINOPOMATOIDEA Bell, 1836
Family? RHINOPOMATIDAE Bonaparte, 1838

Gen. and sp. indet. (Fig. 6).

Referred specimen. **IVPP V18651** (left M^2; Fig. 6A), only known specimen.

Locality and age. Fissure filling A located in the Shanghuang Limestone Quarry, near the village of Shanghuang, Liyang County, southern Jiangsu Province, central coastal China. The locality is correlated with the Sharamurunian Asian Land Mammal Age (ALMA; Russell & Zhai 1987), middle Eocene.

Description. Given the transverse proportions of **IVPP V18651**, this upper tooth is identified here as M^2. The crown is strongly waisted distally. The ectoflexus is situated above the paracone. The dilambdodont ectoloph is well developed (W-shaped, broadly open) and occupies the main part of the tooth. The paracristae are more inclined and longer than the metacristae, thereby rendering the ectoloph asymmetrical. The preparacrista joins a mesially inflected

parastyle. The metastylar shelf differs from the parastyle in being thinner and not curved. The junction between the postparacrista and premetacrista corresponds to a small mesostyle, which occupies a very buccal position. The paracone is bent mesially. This cusp is slightly more voluminous and more buccal than the metacone. A short paraloph extends lingually from the base of the paracone, but it does not join the preprotocrista or the precingulum. The protocone is small and occupies a very mesiolingual position (lingually opposed to the paracone). The postprotocrista is very short and does not close the protofossa distally. In contrast, the preprotocrista is long and joins a strong precingulum, thereby closing the protofossa mesially. The talon basin is moderately extended and appears disjunct from the protofossa, thereby forming a distolingual lobe. The thick lingual cingulum surrounds the distal part of the talon basin and joins a small hypocone, which is situated distolingually to the protocone. A very short crest extends from the mesial base of the hypocone towards the distal wall of the protocone.

Comparison. Extant rhinopomatids are poorly diversified, including only one genus *Rhinopoma*. **IVPP V18651** (1.7 × 1.9; Appendix 1) is medium-sized compared to its counterparts in *Rhinopoma*: *R. hardwickei* (1.42 × 2.03), *R. macinnesi* (1.28 × 1.84), and *R. microphyllum* (1.99 × 2.34) (measurements from Gunnell *et al.* 2008). The M^2 from Shanghuang is referred to the Rhinopomatidae on the basis of its rectangular occlusal outline, its development of a flat talon basin that forms a distolingual lobe, its small protocone with an open protofossa and its minute hypocone. However, **IVPP V18651** shows distinctive features from the rhinopomatid condition, including an ectoflexus over the paracone, a large precingulum, a metacone that is distally inclined and distal waisting of the crown under the metacone. Interestingly, these structures also occur on upper molars of some extant Emballonuridae.

Rhinopomatids are very poorly documented in the fossil record. Gunnell *et al.* (2008) have described one upper molar from the earliest Late Eocene of the Fayum, Egypt (Quarry BQ-2) that could belong to a rhinopomatid (*Qarunycteris moerisae*). **IVPP V18651** from Shanghuang differs from *Qarunycteris* in having a more open ectoloph, a more buccal mesostyle, a wider precingulum, stronger distal waisting of the crown, a shorter postprotocrista, a small hypocone (but well marked) and a more extensive talon basin (lobe). The morphology of *Q. moerisae* is rather similar to some Emballonuridae from the Quercy (such as *Vespertiliavus*), but this unique tooth is not sufficient to clarify its systematic attribution. Fossils attributed to *Rhinopoma* have been described from the Upper Miocene site of Elaiochoria 2 in Chalkidiki, Greece (Hulva *et al.* 2007). The dental morphology of this taxon closely resembles that of extant *Rhinopoma*, except for the hypocone, which is missing in $M^{1\text{-}2}$ of extant *Rhinopoma*.

Suborder MICROCHIROPTERA Dobson, 1875

Fam., gen and sp. indet. (Fig. 6).

Referred specimens. **IVPP V18652** (fragment of dentary bearing P_4; Fig. 6F).

Locality and age. Fissure filling E located in the Shanghuang Limestone Quarry, near the village of Shanghuang, Liyang County, southern Jiangsu Province, central coastal China. The locality is correlated with the Sharamurunian Asian Land Mammal Age (ALMA; Russell & Zhai 1987), middle Eocene.

Description. **IVPP V18652** is a left mandibular fragment preserving the fourth lower premolar (P_4). This tooth is short mesiodistally and oval in occlusal outline. The protoconid is the main cusp of the crown. A low, mesiolingual enamel swelling indicates the presence of a vestigial paraconid. The metaconid is well developed and lingually opposed to the protoconid. A short and rounded talonid, with neither cusps nor crests, extends from the base of the trigonid wall. A moderate but continuous cingulid surrounds the crown buccally. In addition to the preserved P_4, the dentary displays five alveoli: two large alveoli behind the P_4 that would have borne M_1, two additional large alveoli in front of the P_4 for a double-rooted P_3 and a minute alveolus at the front of the preserved part of the jaw. The latter structure suggests the presence of a minute P_2, which is generally well developed in Chiroptera.

Comparison. A dental formula including three premolars indicates a primitive condition for this taxon. The archaic bats from the early Eocene of Vastan in India (Smith *et al.* 2007) have three premolars with a double-rooted P_3 and a single-rooted P_2. **IVPP V18652** displays these characteristics, except for the apparent reduction in P_2. Furthermore, the morphology of P_4 is more advanced than in archaic bats. Indeed, the absence of a strong paraconid, the position of the metaconid and the vestigial talonid contrast with the primitive condition observed in Icaronycteridae and Archaeonycteridae. The P_4 of **IVPP V18652** is more similar to the P_4 of *J. cambayensis* from Vastan. However, **IVPP V18652** differs from the dentary fragments of *J. cambayensis* in being smaller and in having a strongly reduced P_2. *Lapichiropteryx xiei* also has a double-rooted P_3 and a slightly reduced P_2. Compared to the Paleochiropterygidae from central China, **IVPP V18652** is smaller, lacks diastemata between the premolars and has a more reduced P_2. Only a few families of extant bats retain three premolars: the Rhinolophidae, some extinct Hipposi-

deridae, the Phyllostomidae, the Thyropteridae and some Vespertilionidae. The Rhinolophidae and extinct Hipposideridae have a minute, vestigial P_3, which is single-rooted and offset buccally from the rest of the toothrow. This configuration is seen in *P. shanghuangensis* but not in **IVPP V18652**, which has a double-rooted P_3 that seems to have been as large as P_4. Some Phyllostomidae have three premolars, but as in Rhinolophidae and Hipposideridae, it is the P_3 that tends to be reduced. Recent Thyropteridae also retain the third premolar. However, contrary to **IVPP V18652**, all three premolars are single-rooted and relatively homodont. The Vespertilionidae is a particularly well-diversified family, some species of which retain three premolars. In those that do, the second and third premolars are single-rooted and P_2 is slightly larger than P_3.

Cladistic analysis

As *P. shanghuangensis* is only known by isolated teeth and fragments of mandibles, a total of 53 dental characters plus 6 mandibular characters were scored across a set of extinct and extant Chiroptera. Twenty characters were selected on lower teeth and thirty-three on upper teeth (Appendix 2). The selected characters and character states were established from direct observations and comparisons or from the available literature. All characters were equally weighted and unordered.

The selected taxa include the rhinolophoid fossils from Shanghuang and Quercy fissure fillings: *P. shanghuangensis* from the middle middle Eocene of Shanghuang (China; this study), *Vaylatsia prisca* from the early late Eocene (MP17a) to the early Oligocene (MP23) of the Quercy fissure fillings (France; Revilliod 1920; Legendre *et al.* 1995; Sigé *et al.* 1998; Sigé & Crochet 2006; Maitre 2008 [Unpublished PhD]), *Palaeophyllophora oltina* from the middle-late Eocene (MP18) of the Quercy fissure fillings (France; Delfortrie 1872) and *Pseudorhinolophus schlosseri* from the late middle Eocene (MP13) to the early Oligocene (MP22) of the Quercy fissure fillings (France; Revilliod 1917). The other possible rhinolophid (? Rhinolophidae gen and sp. indet.) from Shanghuang was not included in the analysis because of its very limited anatomical documentation, which is restricted to three teeth. The in-group also includes modern species of Rhinolophidae (*Rhinolophus ferrumequinum* and *Rhinolophus hipposideros*) and Hipposideridae (*Hipposideros lankadiva* and *Hipposideros speroris*) to assess the position of the fossils, especially *P. shanghuangensis*, with respect to the Hipposideridae + Rhinolophidae clade. The crown group (Rhinolophidae + Hipposideridae) is rooted using three members of the archaic Chiroptera (i.e. 'Eochiroptera') that constitute the out-group: *Icaronycteris menui* and *Archaeonycteris brailloni* from the early Eocene of the Paris Basin (Russell *et al.* 1973), and *Palaeochiropteryx tupaiodon* from the middle Eocene of Messel, Germany (Russell & Sigé 1970). Characters were polarized via the out-group comparison method (Watrous & Wheeler 1981).

The data matrix is presented in the Appendix 3. The data matrix was managed using NDE (Nexus Data Editor v. 0.5.0; Page 2001). The phylogenetic reconstruction was performed with PAUP* v.4.0 beta 10 Win (Swofford 2002), with an exact search for the most parsimonious tree ('Branch and Bound' option [BandB]). Clade robustness was measured with the Bremer Index and Bootstrap percentages (Felsenstein 1985; Bremer 1994).

Results

The branch-and-bound analysis yielded four equally most parsimonious trees of 118 steps each, with a consistency index (CI) of 0.534 and a retention index (RI) of 0.621. A strict consensus tree is presented in Fig. 7A. According to this tree topology, *P. shanghuangensis* is reconstructed as the basalmost member of the Rhinolophidae. The group also includes *Vaylatsia prisca*, which appears to be the sister group of the two extant rhinolophids (i.e. *Rhinolophus ferumequinum* and *R. hipposideros*). The monophyly of the Rhinolophidae is supported by one unambiguous and non-homoplastic synapomorphy: the presence of a discontinuous lingual cingulum on $M^{1\text{-}2}$ (Ch 51^1; RI = 100). The Hipposideridae form a second major clade characterized by the loss of P_3 (Ch 10^1; RI = 100). This monophyletic group includes the two extant species of *Hipposideros* and *P. schlosseri*. The position of *P. oltina* is not resolved in the strict consensus tree, appearing as a Rhinolophoidea *incertae sedis*. *Palaeophyllophora oltina* is either reconstructed as a stem member of Rhinolophoidea (in two of the four most parcimonious trees) (Fig. 7C) or as the basalmost member of the Hipposideridae (in the two other trees) (Fig. 7B). This latter topology is more congruent with numerous systematic and cladistic studies, which have considered also cranial and postcranial features (e.g. Sigé 1978; Hand 1998a,b; Hand & Kirsch 2003). Assuming the second topology (Fig. 7B), Hipposideridae are characterized by two synapomorphies: the absence of the distolingual lobe on P^4 (Ch 34^1; RI = 50) and the shortening of the postprotocrista, which does not connect the postcingulum (CH 47^1; RI = 100).

Hipposideridae and Rhinolophidae, the twin families

Within the superfamily Rhinolophoidea, the Hipposideridae + Rhinolophidae clade is particularly well supported by a body of morphological and molecular evidence (e.g. Lapointe *et al.* 1999; Levasseur *et al.* 2003; Gunnell & Simmons 2005; Simmons 2005; Teeling *et al.* 2005; Agnarsson *et al.* 2011). Extant Rhinolophidae (horseshoe bats) include

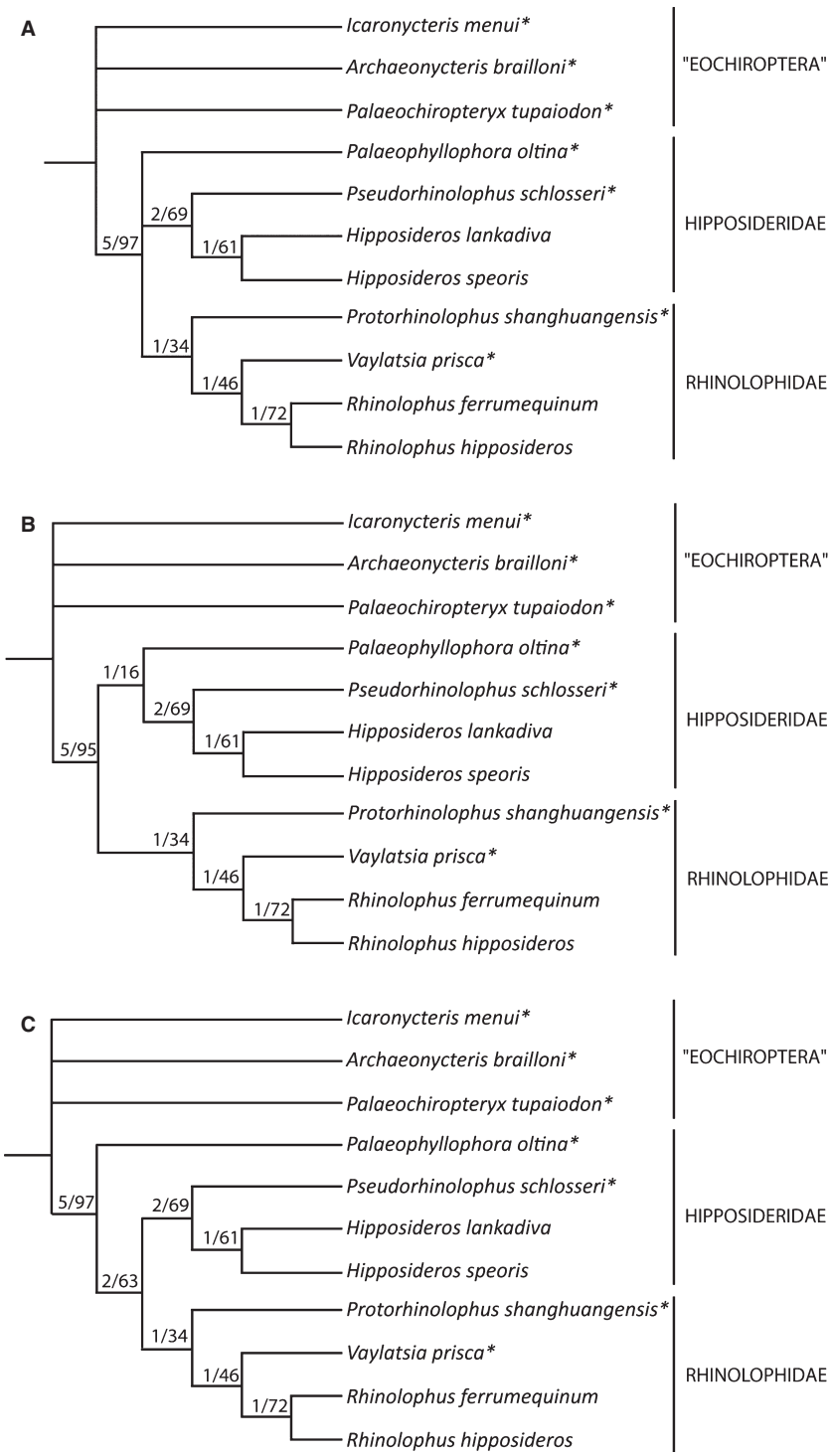

Fig. 7 Phylogenetic hypotheses of rhinolophoid relationship resulting from Branch and Bound analysis conducted on 59 dental characters. —A. Strict consensus of four equally parsimonious trees of 118 steps each with consistency index of 0.534 and retention index of 0.621. —B. Topology found in two of the four most-parsimonious trees. —C. The alternative topology found in two of the four most-parsimonious trees. Phylogenetic analysis was performed with PAUP* v.4.0 beta 10 Win (Swofford 2002). Bremer Index and Bootstrap percentages are given left and right from the slash, respectively.

the single genus *Rhinolophus*, which is the second most speciose genus of Chiroptera, encompassing at least 77 species (Simmons & Conway 2003). In contrast, the Hipposideridae (leaf-nosed, roundleaf and trident bats) encompass a broader range of morphological disparity, which is characterized by nine genera including a total of 65 species (e.g. Koopman 1994; Simmons & Conway 2003). Due to their overall resemblance, the Hipposideridae and Rhinolophidae have long been considered as a single family (e.g. Miller 1907; Simmons & Geisler 1998). Only a few post-

cranial and dental characteristics, the latter being tenuous, have been proposed for distinguishing the two families. Miller (1907) distinguished the Hipposideridae from the Rhinolophidae essentially on the basis of postcranial characteristics. Indeed, hipposiderids differ from rhinolophids in having 'pectoral and pelvic girdles, more highly modified, toes with two phalanges each, and lumbar vertebrae showing a marked tendency to become into a solid rod' (Miller 1907; p. 109). In addition, rhinolophids are also characterized by the distal articulation of the humerus, which allows for more specialized flight (Sigé 1978, 1990). Regarding the dentition, extinct and extant rhinolophids have a vestigial P_3, which is lost in all extant hipposiderids. Furthermore, some hipposiderids (*Hipposideros*, *Anthops* and *Asellia*) have their M^3 and M_3 strongly reduced compared to rhinolophids. More recently, molecular and morphological phylogenetic investigations have brought strong support for considering the Hipposideridae and Rhinolophidae as two distinct natural groups (e.g. Bogdanowicz & Owen 1998; Hand & Kirsch 1998; Wang *et al.* 2004; Eick *et al.* 2005; Simmons 2005; Eiting & Gunnell 2009), which seem to have diverged during the middle Eocene (ca. 39 Mya) from an Asian common ancestor (Teeling *et al.* 2005). With respect to the fossil record of the two families, rhinolophids are less known in the early Tertiary than hipposiderids. *Rhinolophus priscus*, which is recorded from the late Eocene to the Oligocene in the Quercy of France (Sigé 1978), represents the oldest known occurrence of the Rhinolophidae. Several other indeterminate species of *Rhinolophus* are found in the Paleogene of Europe, notably in the late Oligocene of Carrascosa in central Spain (Sevilla 1990). Fossils of hipposiderids are thought to be more abundant and to have a broader distribution. Eighteen species distributed among the genera *Hipposideros* (*Pseudorhinolophus*), *Palaeophyllophora* and *Vaylatsia* (the latter of which we regard as a member of Rhinolophidae) are present in the fissure fillings of Western Europe (France) from the end of the middle Eocene to the end of the Oligocene (e.g. Sigé 1978, 1990, 1997; Sigé & Legendre 1983). Hipposiderids are also documented in the early Oligocene of the Sultanate of Oman with *Hipposideros* (*Brachipposideros*) *omani* and another indeterminate species (Sigé *et al.* 1994). Like extant and extinct *Rhinolophus*, the Paleogene genera *Palaeophyllophora* and *Vaylatsia* retain primitive dental structures that are lost in *Hipposideros*. Furthermore, the dentition of *Vaylatsia* does not differ substantially from that of *Rhinolophus*. Although the dental morphology of *Vaylatsia* strongly resembles that of Rhinolophidae, this fossil bat has been regarded as a stem member of Hipposideridae based primarily on referred humeri, which show a typical hipposiderid morphology. Despite this, the strong dental and mandibular similarities between *Vaylatsia* and *Rhinolophus* led Sigé (1990) to suggest that these taxa could be closely related. However, the fissure filling (Garouillas, MP25, middle Oligocene: Sigé 1990) from which *Vaylatsia garouillasensis* has been described on the basis of abundant dental material and humeri has also yielded several specimens of *Hipposideros* (*Pseudorhinolophus*) *zbrjdi*. Given that *Vaylatsia* and *Hipposideros* are roughly similar in size, the possibility exists that the hipposiderid humeri attributed to *Vaylatsia* actually belong to *Hipposideros*. As such, because the hipposiderid status of *Vaylatsia* relies primarily on these attributed humeri, the dental morphology of this fossil bat suggests that it might better be interpreted as a basal member of Rhinolophidae. Indeed, our phylogenetic results indicate that *Vaylatsia* is clearly nested within the Rhinolophidae (Fig. 7).

With the presence of a vestigial P_3, a hypoconulid displaced buccally on the lower molars, and upper molars with a closed protofossa and well-developed talon, *P. shanghuangensis* from Shanghuang strongly resembles *Vaylatsia*. However, in some dental traits, *Protorhinolophus* appears to be more primitive than *Vaylatsia*. This is particularly the case with respect to the upper molars ($M^{1\text{-}2}$), which have a mesostyle that is still very buccal in position and a strongly projecting distolingual shelf. The P_3 in *Protorhinolophus* is also less reduced than in *Vaylatsia*. However, given the greater antiquity of *Protorhinolophus* (middle Eocene) with respect to *Vaylatsia* (late middle Eocene to basal early Oligocene), the primitive dentition of the former taxon *Protorhinolophus*is hardly surprising. Interestingly, as we have discussed earlier, the dental pattern of *Protorhinolophus* shows a mosaic of primitive and derived features ('Eochiroptera' *vs* Rhinolophidae dental characteristics) that indicate a basal phylogenetic position for this taxon within the Rhinolophidae (Fig. 7). Assuming that *Protorhinolophus* is a stem rhinolophid and the most ancient representative of the family, the presence of this taxon at Shanghuang testifies to the great antiquity of the Rhinolophidae in Asia, thereby suggesting a possible Asian origin of this clade. Given that *Rhinolophus* is recorded only from the middle-late Eocene in Europe (i.e. *Rhinolophus priscus*; Sigé 1978) and that *Vaylatsia* is recorded as early as the late middle Eocene [i.e. *V. astruci* and *V. cregolensis*; Maitre 2008 (Unpublished PhD)], the arrival of Rhinolophidae in western Europe may reflect their dispersal from Asia during the late middle Eocene (Fig. 8). However, this case of dispersal contrasts with the provincialism effect of Shanghuang during the middle Eocene advocated by Métais *et al.* (2008). This isolation is marked by a warm and dry climate that contrasts with the tropical climate of the inner continent. Presumably, bats are more capable of dispersal because their ability to fly confers an obvious advantage to them in traversing great distances and crossing geographic

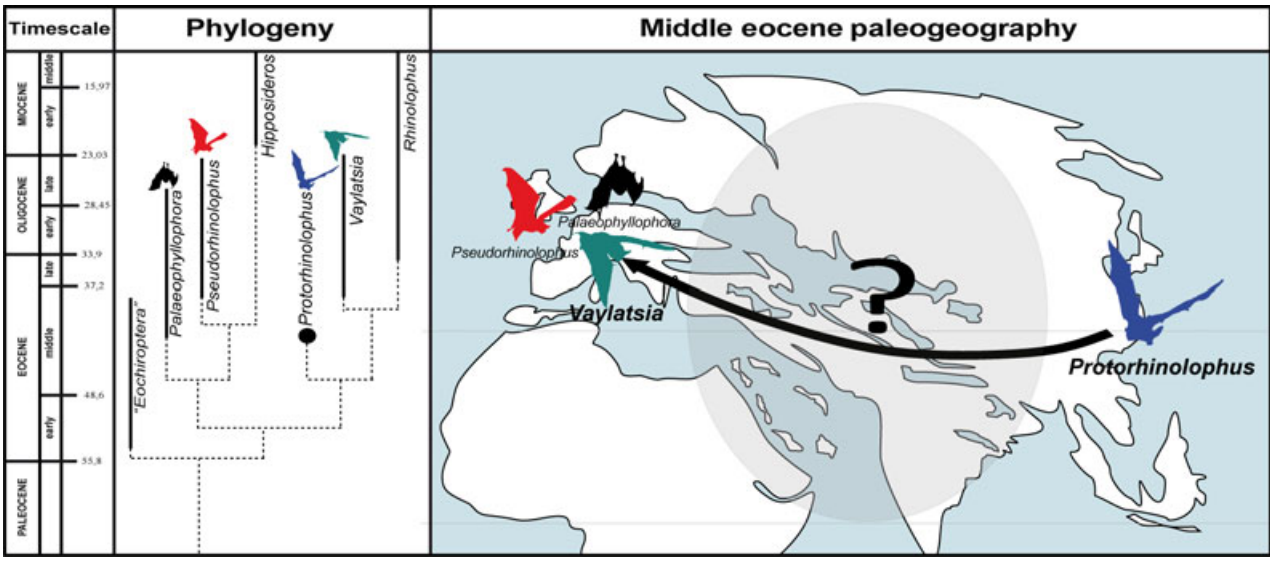

Fig. 8 Phylogeographic hypothesis for early Rhinolophidae during the middle Eocene. Timescale is shown at the left of the figure. The phylogenetic hypothesis is taken from the alternative tree scored after Branch and Bound analysis (Fig. 6B). Hypothesized dispersal event is shown on the right. The arrow shows the probable dispersal pathway of early Rhinolophidae. The question mark emphasizes the gap in the fossil record between the two areas and during the Paleogene.

barriers. Furthermore, the early Asian migration towards Europe was supported for the adapine primates suggesting that climatic zonation of China have not affected all mammalian group as a same way during the middle Eocene (Beard *et al.* 1994).

The early evolutionary history of Rhinopomatidae

Because of the great similarity in dental morphology between Rhinopomatidae and Emballonuridae, in the absence of a more comprehensive fossil record, the systematic attribution of the upper molar **IVPP V18651** remains uncertain. The lingual part of this tooth is very compressed buccolingually, as is the case in upper teeth of rhinopomatids (i.e. *Rhinopoma*). With such a lingual structure, **IVPP V18651** diverges substantially from upper molars of the Emballonuridae, which have a better developed protocone and a more extensive talon basin that is directly connected to the protofossa. However, the deeply mesially indented buccal edge structure observed in **IVPP V18651** is not found in upper teeth of rhinopomatids, although this structure resembles that found in molars of emballonurids, notably *Vespertiliavus* from the middle Eocene to late Oligocene of Europe.

The Rhinopomatidae (mouse-tailed bats) are generally viewed as one of the most ancient families of modern Chiroptera (Valen 1979; Simmons 2005; Hulva *et al.* 2007). Today, this family is restricted to a single genus (*Rhinopoma*) with only four species (*R. hardwickii*, *R. microphyllum*, *R. muscatellum* and *R. hadramauticum*), which have a widespread distribution over the Old World, especially in northern Africa, peninsular Arabia, the eastern Mediterranean and Indo-Pakistan. Despite its early emergence, this modern bat group is extremely poorly documented in the fossil record. *Qarunycteris moerisae*, documented by a single tooth from the earliest late Eocene of Egypt (Fayum, BQ2; Gunnell *et al.* 2008), is currently considered to be the oldest representative of the family. The other record of the family is from the upper Miocene Elaiochoria site in Greece (Chalkidiki; Hulva *et al.* 2007), which has yielded dental remains of a taxon showing strong affinities with the extant species *R. hardwickii* (*R.* aff. *hardwickii*). If **IVPP V18651** proves to be a member of the Rhinopomatidae, this taxon from Shanghuang would become the oldest occurrence of the family, extending their record back to the middle middle Eocene.

Modern bat radiation

The new Shanghuang bats described here reveal a prevalence of modern families that contrasts with the archaic bat fauna from the early Eocene of India. Contrary to the situation in Europe, Africa and North America, prior to this report Asia lacked any representatives of modern microchiropteran superfamilies or families during the Paleogene, with the possible exception of *J. cambayensis* (Smith *et al.* 2007). In lacking 'Eochiroptera', the Shanghuang bat fauna emphasizes the existence of a turnover in Asian bat communities that seems to have occurred during the middle Eocene. Rhinolophoids appear dominant and show a com-

bination of plesiomorphies and apomorphies marking a transition between 'Eochiroptera' and modern families. The modern bat radiation remains an enigmatic and complex event that seems to have occurred in various ways on each continent. The modern bat families appeared in the fossil record as early as the late early Eocene on several continents (North America, Europe and Africa) and radiate during the middle Eocene, while archaic bats ('Eochiroptera') become progressively rare (e.g. Simmons & Geisler 1998; Gunnell & Simmons 2005; Simmons 2005; Eiting & Gunnell 2009). To date, among the oldest microchiropteran faunas, Europe has yielded one of the oldest assemblages of modern forms, notably from the middle Eocene French karstic infillings (Quercy). The fossils include members of the extant families Rhinolophidae, Hipposideridae and Emballonuridae (Sigé 1978, 1990, 1997; Sigé & Legendre 1983). The Mixopterygidae are also included in the modern European radiation of bats, but the phylogenetic position of this extinct group remains unclear (Maitre *et al.* 2008). In addition, Europe documents one of the oldest representatives of an extant microchiropteran family: *Tachypteron franzeni* from the middle Eocene of Messel (Germany), which is described as a primitive Emballonuridae (Storch *et al.* 2002). Given the early diversification of this extant family, Storch *et al.* (2002) proposed a pre-middle Eocene radiation for the modern bats and particularly for the emballonuroids. Africa is known for including several modern bats during the Eocene. The locality of Chambi in Tunisia documents the late early Eocene extinct Philisidae (*Dizzya exsultans*), which is thought to be a primitive member of Vespertilionoidea (Sigé 1991), as well as other modern groups such as Emballonuroidea (Emballonuridae), Rhinolophoidea (Hipposideridae) and other Vespertilionoidea (Ravel *et al.* 2011, 2012; Ravel 2012 [Unpublished PhD]). In addition, the abundant dental remains from the late Eocene of the Fayum in Egypt document exclusively modern taxa including Vespertilionidae, Rhinopomatidae, Philisidae and Emballonuridae. The early diversity of microbats in Africa during the Eocene could support an African origin for some modern families as suggested by Sigé (1991). A member of the modern family Natalidae, *Honrovits tsuwape*, is reported from the late early Eocene (Lostcabinian, late Wasatchian; Beard *et al.* 1992) of central Wyoming in North America, which could represent the oldest representative of this family. However, this taxon was recently reconsidered and placed among the Onychonycteridae owing to its similar dental morphology with the most primitive bat *Onychonycteris finneyi* (Smith *et al.* 2012). With the occurrence of Vespertilionoidea (Philisidae), Emballonuroidea and Hipposideridae in the late early Eocene of North Africa (Chambi), Emballonuridae in the earliest Eocene of England (Abbey Wood), Natalidae in the late early Eocene of North America (Wyoming), Rhinolophidae and a possible Rhinopomatidae in the middle middle Eocene of China (Shanghuang), it is clear that modern bats were already well diversified as early as the early Eocene with a widespread distribution.

Conclusion

The new bat assemblage from the middle Eocene of Shanghuang documents a stem member of Rhinolophidae, two indeterminate rhinolophoids, and a possible member of Rhinopomatidae, representing the oldest occurrences of these modern families in Asia. *Protorhinolophus shanghuangensis* gen. and sp. n. show close affinities with *Vaylatsia* from France, suggesting dispersal of the first rhinolophids from Asia to western Europe during the middle Eocene. These discoveries contribute to a better understanding of the modern bat radiation in Asia, although the temporal and spatial gaps that remain in the Asian bat fossil record continue to obscure our knowledge of their early evolutionary history.

Among the bat species from Shanghuang, one is well represented (*P. shanghuangensis*) by approximately 80% of known specimens, which strongly suggests the possibility that this taxon inhabited caves. In contrast, very few specimens represent the three other species. The biased taxonomic documentation is surprising for a karstic locality such as Shanghuang, which usually preserve a diversified and abundant bat fauna (Kowalski 1995). This uneven documentation could be explained either by biased sampling of the fossils or by an absence of cave habitation among the underrepresented species. Taphonomy can be a good indication of palaeoecology and roosting behaviour in fossil bats. The stem-chiropterans ('Eochiroptera') are often found in fluvio-lacustrine deposits, while modern forms appear essentially in karstic deposits (e.g. Sigé & Legendre 1983). The new bat fauna from Shanghuang is essentially composed of modern taxa, thereby conforming this tendency. The Shanghuang bat fauna could therefore reflect the early appearance of cave habitation among modern bats in Asia.

Acknowledgements

The authors are very grateful to Allan Tabrum for his help in preparation of the fossils. Special thanks are extended to Pauline Coster for having taken SEM pictures of the specimens figured in this work. Field research was supported by grants from the US National Science Foundation (most recently, BCS 0820602) and the National Basic Research Program of China (2012CB821904). Other financial suport was also provided by the French ANR-ERC PALASIAFRICA Program (ANR-08-JCJC-0017). This is ISE-M publication 2013-085.

References

Agnarsson, I., Zambrana-Torrelio, C. M., Flores-Saldana, N. P. & May-Collado, L. J. (2011). A time calibrated species-level phylogeny of bats (Chiroptera, Mammalia). *PloS Currents*. Tree of Life 3.

Beard, K. C., Sigé, B. & Krishtalka, L. (1992). A primitive vespertilionoid bat from the Early Eocene of central Wyoming. *Compte rendu de l'Académie des Sciences de Paris*, *314*, 735–741.

Beard, K. C., Qi, T., Dawson, M. R., Wang, B. & Li, C. (1994). A diverse new primate fauna from the Middle Eocene fissure-fillings in southeastern China. *Nature*, *368*, 604–609.

Beard, K. C., Tong, Y., Dawson, M. R., Wang, J. & Huang, X. (1996). Earliest complete dentition of an anthropoid primate from the late Middle Eocene of Shanxi Province, China. *Science*, *272*, 82–85.

Berggren, W. A. & Prothero, D. R. (1992). Eocene-Oligocene climatic and biotic evolution: an overview. In W. A. Berggren & D. R. Prothero (Eds) *Eocene-Oligocene Climatic and Biotic Evolution* (pp. 1–28). Princeton, NJ: Princeton University Press.

Bogdanowicz, W. & Owen, R. D. (1998). In the Minotaur's labyrinth: the phylogeny of the bat family Hipposideridae. In T. H. Kunz & P. A. Racey (Eds) *Bat Biology and Conservation* (pp. 27–42). Washington, DC: Smithsonian Institution Press.

Bremer, K. (1994). Branch support and tree stability. *Cladistics*, *10*, 295–304.

Dawson, M. R. & Wang, B. (2001). Middle Eocene Ischyromyidae (Mammalia: Rodentia) from the Shanghuang fissures, southeastern, China. *Annals of Carnegie Museum of Natural History*, *70*, 221–230.

Dawson, M. R., Huang, X., Li, C. & Wang, B. (2003). Zelomyidae, a new family of Rodentia (Mammalia) from the Eocene of Asia. *Vertebrata Palasiatica*, *41*, 249–270.

Delfortrie, E. (1872). Les gites de chaux phosphatée dans le département du Lot; leur faune, le mode et l'époque probable de leur formation. *Actes de la Société Linnéenne de Bordeaux*, *28*, 505–518.

Ducrocq, S., Jaeger, J.-J. & Sigé, B. (1993). Un mégachiroptère dans l'Eocène supérieur de Thaïlande: incidence dans la discussion phylogénique du groupe. *Neues Jahrbuch für Geologie und Paläontologie*, *9*, 561–575.

Eick, G. N., Jacobs, D. S. & Mathee, C. A. (2005). A nuclear DNA phylogenetic perspective on the evolution of echolocation and historical biogeography of extant bats (Chiroptera). *Molecular Biology and Evolution*, *22*, 1869–1886.

Eiting, T. P. & Gunnell, G. F. (2009). Global completeness of bat fossil record. *Journal of Mammalian Evolution*, *16*, 151–173.

Felsenstein, J. (1985). Confidence limits on phylogenies: an approach using bootstrap. *Evolution*, *39*, 783–791.

Gunnell, G. F. & Simmons, N. B. (2005). Fossil evidence and the origin of bats. *Journal of Mammalian Evolution*, *12*, 209–246.

Gunnnell, G., Simons, E. L. & Seiffert, E. R. (2008). New bats (Mammalia: Chiroptera) from the late Eocene and early Oligocene, Fayum depression, Egypt. *Journal of Vertebrate Paleontology*, *28*, 1–11.

Guo, J., Dawson, M. R. & Beard, K. C. (2000). *Zhailimeryx*, a new lophiomerycid artiodactyl (Mammalia) from the late Middle Eocene of Central China and the early evolution of ruminants. *Journal of Mammalian Evolution*, *7*, 239–258.

Habersetzer, J. & Storch, G. (1987). Klassifikation und funktionelle flügelmorphologie paläogener fledermäus (Mammalia, Chiroptera). *Courier Forschungsinstitut Senckenberg*, *91*, 117–150.

Hand, S. (1998a). *Xenorbinos*, a new genus of old world leaf-nosed bats (Microchiroptera: Hipposideridae) from the Australian Miocene. *Journal of Vertebrate Paleontology*, *18*, 430–439.

Hand, S. (1998b). *Riversleigha williamsi* gen. et sp. nov., a large Miocene hipposiderid (Microchiroptera) from Riversleigh, Queensland. *Alcheringa*, *22*, 259–276.

Hand, S. & Kirsch, J. A. W. (1998). A Southern origin for the Hipposideridae (Microchiroptera)? Evidence from the Australian fossil record. In T. H. Kunz & P. A. Racey (Eds.) *Bats: Phylogeny, Morphology, Echolocation, and Conservation Biology* (pp. 72–90). Washington, DC: Smithsonian Institution Press.

Hand, S. & Kirsch, J. A. W. (2003). Archerops, a new annectent hipposiderid genus (Mammalia: Microchiroptera) from the Australian Miocene. *Journal of Paleontology*, 77, 1139–1151.

Hulva, P., Horacek, I. & Benda, P. (2007). Molecules, morphometrics and new fossils provide an integrated view of the evolutionary history of Rhinopomatidae (Mammalia: Chiroptera). *BMC Evolutionary Biology*, 7, 1–15.

Koopman, K. F. (1994). Chiroptera: systematics. Handbook of zoology. *Mammalia VIII*, *60*, 1–217.

Kowalski, K. (1995). Taphonomy of bats (Chiroptera). *Geobios*, *18*, 251–256.

Lapointe, F.-J., Kirsch, J. A. W. & Hutcheon, J. M. (1999). Total evidence, consensus, and bat phylogeny: a distance-biased approach. *Molecular Phylogenetics and Evolution*, *11*, 55–66.

Legendre, R.-S., Marandat, B., Remy, J. A., Sigé, B., Sudre, J., Vianey-Liaud, M., Crochet, J.-Y. & Godinot, M. (1995). Coyrou 1-2, une nouvelle faune de mammifères des Phosphorites du Quercy, niveau intermédiaire (MP 20-21) proche de la "Grande Coupure". *Géologie de la France*, *1*, 63–68.

Levasseur, C., Landry, P.-A., Makarenkov, V., Kirsch, J. A. W. & Lapointe, F.-J. (2003). Incomplete distance matrices, supertrees and bat phylogeny. *Molecular Phylogenetics and Evolution*, *27*, 239–246.

Maitre, E. (2008). Les chiroptères paléokarstiques d'Europe occidentale, de l'Eocène moyen à l'Oligocène inférieure, d'après les nouveaux matériaux du Quercy (SW France): systématique, phylogénie, paléobiologie. Unpublished thesis. Lyon: Université Claude Bernard-Lyon 1.

Maitre, E., Sigé, B. & Escarguel, G. (2008). A new family of bats in the Paleogene of Europe: systematics and implications for the origin of emballonurids and rhinolophoids. *Neues Jahrbuch für Geologie und Paläontologie – Abhandlugen*, *250*, 199–216.

Métais, G., Guo, J. & Beard, K. C. (2004). A new small dichobunid artiodactyl from Shanghuang (middle Eocene, eastern China): implications for the early evolution of proto-selenodonts in Asia. *Bulletin of Carnegie Museum of Natural History*, *36*, 177–197.

Métais, G., Qi, T., Guo, J. & Beard, K. C. (2005). A new bunoselenodont artiodactyl from the middle Eocene of China and the early record of selenodont artiodactyls in Asia. *Journal of Vertebrate Paleontology*, *25*, 994–997.

Métais, G., Qi, T., Guo, J. & Beard, K. C. (2008). Middle Eocene artiodactyls from Shanghuang (Jiangsu Province, Coastal China) and the diversity of basal dichobunoids in Asia. *Naturwissenschaften*, *95*, 1121–1135.

Miller, G. S. (1907). *The Families and Genera of Bats*. Bulletin 57 of the United States National Museum, Washington, DC: Smithsonian Institution Press, 282 pp.

Qi, T. & Beard, K. C. (1996). *Nanotitan Shanghuangensis*, gen. et sp. nov.: the smallest known brontothere (Mammalia: Perissodactyla). *Journal of Vertebrate Paleontology*, *16*, 578–581.

Qi, T., Zong, G. & Wang, Y. (1991). Discovery of *Lushilagus* and *Miacis* in Jiangsu and its zoogeographical significance. *Vertebrata Palasiatica*, *29*, 59–63.

Qi, T., Beard, K. C., Wang, B., Dawson, M. R., Guo, J. & Li, C. (1996). The Shanghuang mammalian fauna, Middle Eocene of Jiangsu: history of discovery and significance. *Vertebrata Palasiatica*, *34*, 202–214.

Rana, R. S., Singh, H., Sahni, A., Rose, K. D. & Saraswati, P. K. (2005). Early Eocene chiropterans from a new mammalian assemblage (Vastan Lignite Mines, Gujarat, western peninsular margin): oldest known bats from Asia. *Journal of the Palaeontological Society of India*, *50*, 93–100.

Ravel, A., Marivaux, L., Tabuce, R., Adaci, M., Mahboubi, M., Mebrouk, F., Bensalah, M., Ben Haj Ali, M., Essid, E. M. & Vianey-Liaud, M. (2011). Eocene Chiroptera from Tunisia and Algeria: new insight into the early evolution of bats in North Africa. In T. Lehmann & S. F. K. Schaal (Eds) *The World at the Time of Messel* (pp. 139). Frankfurt: Mosbrugger, H. C. Volker Senckenberg Research Institute and Natural History Museum Frankfurt.

Ravel, A., Marivaux, L., Tabuce, R., Ben Haj Ali, M. & Essid, E. M. (2012). A new large philisid (Mammalia, Chiroptera, Vespertilionoidea) from the late Early Eocene of Chambi, Tunisia. *Palaeontology*, *55*, 1034–1041.

Revilliod, P. (1917). Contribution à l'étude des chiroptères des terrains tertiaires. *Mémoires de la Société Paléontologique Suisse*, *43*, 1–58.

Revilliod, P. (1920). Contribution à l'étude des chiroptères des terrains tertiaires. 2. *Mémoire de la société paléontologique suisse*, *44*, 63–128.

Russell, D. E. & Gingerich, P. D. (1981). Lipotyphla, Proteutheria (?), and Chiroptera (Mammalia) from the Early-Middle Eocene Kuldana Formation of Kohat (Pakistan). *Contributions from the Museum of paleontology, The University of Michigan*, *25*, 277–287.

Russell, D. E. & Sigé, B. (1970). Révision des chiroptères lutétiens de Messel (Hesse, Allemagne). *Palaeovertebrata*, *3*, 83–182.

Russell, D. E. & Zhai, R.-J. (1987). The Paleogene of Asia: mammals and stratigraphy. *Mémoires du Muséum d'Histoire Naturelles (Série C, Sciences de la Terre)*, *52*, 1–488.

Russell, D. E., Louis, P. & Savage, D. E. (1973). Chiroptera and Dermoptera of the French Early Eocene. *University of California Publications in Geological Sciences*, *95*, 1–57.

Sevilla, P. (1990). Rhinolophoidea (Chiroptera, Mammalia) from the upper Oligocene of Carrascosa del Campo (Central Spain). *Geobios*, *23*, 173–188.

Sigé, B. (1978). La poche à phosphate de Ste-Néboule (Lot) et sa faune de vertébrés du Ludien supérieur. *Palaeovertebrata*, *8*, 249–268.

Sigé, B. (1990). Nouveaux chiroptères de l'Oligocène moyen des phosphorites du Quercy, France. *Compte rendu de l'Académie des Sciences de Paris*, *310*, 1131–1137.

Sigé, B. (1991). Rhinolophoidea et Vespertilionoidea (Chiroptera) du Chambi (Eocène inférieur de Tunisie). Aspect biostratigraphique, biogéographique et paléoécologique de l'origine des chiroptères modernes. *Neues Jahrbuch für Geologie und Paläontologie – Abhandlugen*, *182*, 355–376.

Sigé, B. (1997). Les remplissages karstiques polyphasés (Eocène, Oligocène, Pliocène) de Saint-Maximin (phosphorite du Gard) et leur apport à la connaissance des faunes européennes, notamment pour l'Eocène moyen (Mp13). 3-Systématique: euthériens entomophages. In J.-P. Aguilar, R.-S. Legendre & J. Michaux (Eds) *Actes du Congrès BiochroM'97* (pp. 737–750). Montpellier: Mémoires et Travaux de l'Ecole pratique des Hautes Études, Institut de Montpellier.

Sigé, B. & Crochet, J.-Y. (2006). Marsupiaux, insectivores s.l., chiroptères, créodontes et carnivores paléogènes d'Europe décrits ou révisés d'après les nouvelles collections du Quercy (SW France). In T. Pélissié & B. Sigé (Eds) *Strata vol. 13 : 30 millions d'années de biodiversité dynamique dans le paléokarst du Quercy* (pp. 189–205). Toulouse: Association Strata, Journées Bernard Géze, Lalbenque-Limogne.

Sigé, B. & Legendre, R.-S. (1983). L'histoire des peuplements de chiroptères du bassin méditerranéen: l'apport comparé des remplissages karstiques et des dépôts fluvio-lacustres. *Mémoire Biospéologique*, *10*, 209–225.

Sigé, B., Thomas, H., Sen, S., Gheerbrant, E., Roger, J. & Al-Sulaimani, Z. (1994). Les chiroptères de Taqah (Oligocène inférieur, Sultanat d'Oman). Premier inventaire systématique. *Münchner Geowissenschaftliche Abhandlungen*, *26*, 35–48.

Sigé, B., Hugueney, M., Crochet, J.-Y., Legendre, R.-S., Mourer-Chauviré, C., Rage, J.-C. & Simon-Coiçon, R. (1998). Baraval, nouvelle faune de l'Oligocène inférieur (MP22) des Phosphorites du Quercy. Apport à la signification chronologique des remplissages karstiques. *Bulletin de la Société d'Histoire Naturelle de Toulouse*, *134*, 85–90.

Simmons, N. B. (2005). Chiroptera. In K. D. Rose & J. D. Archibald (Eds) *The Rise of Placental Mammals: Origins and Relationships of the Major Extant Clades* (pp. 159–173). Baltimore, MD: The Johns Hopkins University Press Baltimore.

Simmons, N. B. & Conway, T. M. (2003). Evolution of ecological diversity in bats. In . H. Kunz & M. B. Fenton (Eds) *Bat ecology* (pp. 493–535). Chicago, IL: The University of Chicago.

Simmons, N. B. & Geisler, J. H. (1998). Phylogenetic relationship of *Icaronycteris*, *Archaeonycteris*, *Hassianycteris*, and *Palaeochiropteryx* to extant bat lineages, with comments on the evolution of echolocation and foraging strategies in Microchiroptera. *Bulletin of the United States National Museum*, *235*, 1–182.

Smith, T., Rana, R. S., Missiaen, P., Rose, K. D., Sahni, A., Singh, H. & Singh, L. (2007). High bat (Chiroptera) diversity in the Early Eocene of India. *Naturwissenschaften*, *94*, 1003–1009.

Smith, T., Habersetzer, J., Simmons, N. B. & Gunnell, G. F. (2012). Systematics and paleobiogeography of early bats. In G. F. Gunnell & N. B. Simmons (Eds) *Evolutionary History of Bats: Fossils, Molecules and Morphology* (pp. 23–66). Cambridge: Cambridge University Press.

Springer, M. S., Teeling, E. C., Madsen, O., Stanhope, M. J. & Jong, W. W. (2001). Integrated fossil and molecular data reconstruct bat echolocation. *Proceedings of the National Academy of Sciences*, *98*, 6241–6246.

Storch, G., Sigé, B. & Habersetzer, J. (2002). *Tachypteron franzeni* n. gen., n. sp., earliest emballonurid bat from the Middle Eocene of Messel (Mammalia, Chiroptera). *Paläeontologische Zeitschrift*, *76*, 189–199.

Swofford, D. L. (2002). *PAUP – Phylogenetic Analysis Using Parsimony (*and other methods)*, *Vol. Version 4.0 [Computer Software and Manual]*. Sunderland, MA: Sinauer Associates.

Szalay, F. S. (1969). Mixodectidae, Microsyopidae, and the insectivore-primate transition. *Bulletin of American Museum of Natural History*, *140*, 163–330.

Teeling, E. C., Springer, M. S., Madsen, O., Bates, P., O'Brien, S. J. & Murphy, W. J. (2005). A molecular phylogeny for bats illuminates biogeography and the fossil record. *Science*, *307*, 580–584.

Tong, Y. (1997). Middle Eocene small mammals from Liguanqiao Basin of Henan Province and Yuanqu Basin of Shanxi Province, Central China. *Palaeontologica Sinica*, *18*, 26–256.

Tong, Y., Zheng, S. & Qiu, Z. (1995). Cenozoic mammal ages of China. *Vertebrata Palasiatica*, *33*, 290–314.

Valen, L. V. (1966). Deltatheridia, a new order of mammals. *Bulletin of the American Museum of Natural History*, *132*, 1–125.

Valen, L. V. (1979). The evolution of Bat. *Evolutionary Theory*, *4*, 103–121.

Wang, B. & Dawson, M. R. (1994). A primitive cricetid (Mammalia, Rodentia) from the middle Eocene of Jiangsu province, China. *Annals of Carnegie Museum of Natural History*, *63*, 239–256.

Wang, D., Oakley, T., Mower, J., Shimmin, L. C., Yim, S., Honeycutt, R. L., Tsao, H. & Li, W.-H. (2004). Molecular evolution of bat color vision genes. *Molecular Biology and Evolution*, *21*, 295–302.

Watrous, L. E. & Wheeler, Q. D. (1981). The out-group comparison method of character analysis. *Systematic Biology*, *30*, 1–11.

Appendix 1: Dental measurements of chiropterans from the middle Eocene of Shanghuang fissure fillings (China).

Taxon	Fissure	Specimen	Tooth	L	w	H	Figures
Protorhinolophus shanghuangensis	Shanghuang fissure A	IVPP V18643	Right dentary with p_4-m_3	11.77	2.85		Figs 3B and 4F
Protorhinolophus shanghuangensis	Shanghuang fissure A	IVPP V18644.1	Left toothless dentary	12.79	2.58		Figs 3A and 4G
Protorhinolophus shanghuangensis	Shanghuang fissure A	IVPP V18644.9	Right c_1	1.07	0.84		
Protorhinolophus shanghuangensis	Shanghuang fissure A	IVPP V18644.8	Right c_1	1.18	0.99	2.16	Fig. 4J
Protorhinolophus shanghuangensis	Shanghuang fissure A	IVPP V18644.10	Right c_1	1.13	0.98		
Protorhinolophus shanghuangensis	Shanghuang fissure C	IVPP V18648.1	Right c_1	1.29	1.06	2.2	
Protorhinolophus shanghuangensis	Shanghuang fissure A	IVPP V18644.2	Left c_1	1.16	0.85	1.84	
Protorhinolophus shanghuangensis	Shanghuang fissure A	IVPP V18644.3	Left c_1	1.06	0.89	1.84	
Protorhinolophus shanghuangensis	Shanghuang fissure A	IVPP V18644.4	Left c_1	1.22	1.04	2.28	
Protorhinolophus shanghuangensis	Shanghuang fissure A	IVPP V18644.5	Left c_1	1.06	0.85	1.79	
Protorhinolophus shanghuangensis	Shanghuang fissure A	IVPP V18644.6	Left c_1	1.11	0.89	1.81	
Protorhinolophus shanghuangensis	Shanghuang fissure A	IVPP V18644.7	Left c_1	1.18	1.05	2.11	
Protorhinolophus shanghuangensis	Shanghuang fissure B	IVPP V18645.1	Left c_1	1.19	0.92	1.63	
Protorhinolophus shanghuangensis	Shanghuang fissure E	IVPP V18646.1	Left c_1	1.22	1.02		
Protorhinolophus shanghuangensis	Shanghuang fissure D	IVPP V18647.1	Right p_2	1.01	0.9		
Protorhinolophus shanghuangensis	Shanghuang fissure D	IVPP V18647.2	Left p_2	0.96	0.95		
Protorhinolophus shanghuangensis	Shanghuang fissure E	IVPP V18646.2	Left p_2	0.86	0.82		Fig. 4K
Protorhinolophus shanghuangensis	Shanghuang fissure A	IVPP V18644.11	Left p_2	1.06	0.73		Fig. 4L
Protorhinolophus shanghuangensis	Shanghuang fissure A	IVPP V18644.13	Right p_4	1.28	0.9		
Protorhinolophus shanghuangensis	Shanghuang fissure A	IVPP V18644.14	Right p_4	1.32	0.87		Fig. 4N
Protorhinolophus shanghuangensis	Shanghuang fissure A	IVPP V18644.12	Left p_4	1.33	0.86		Fig. 4M
Protorhinolophus shanghuangensis	Shanghuang fissure B	IVPP V18645.2	Left p_4	1.26	0.86		
Protorhinolophus shanghuangensis	Shanghuang fissure A	IVPP V18644.15	Right m_1	1.82	1.18		Fig. 4O
Protorhinolophus shanghuangensis	Shanghuang fissure E	IVPP V18646.3	Left m_1	1.92	1.26		
Protorhinolophus shanghuangensis	Shanghuang fissure A	IVPP V18644.34	Left m_2	1.75	1.16		
Protorhinolophus shanghuangensis	Shanghuang fissure D	IVPP V18647.3	Left m_2	1.75	1.34		Fig. 4P
Protorhinolophus shanghuangensis	Shanghuang fissure E	IVPP V18646.4	Left m_2	1.85	1.1		
Protorhinolophus shanghuangensis	Shanghuang fissure A	IVPP V18644.16	Left m_3	1.33	0.88		
Protorhinolophus shanghuangensis	Shanghuang fissure B	IVPP V18645.3	Left m_3	1.67	1.06		Fig. 4Q
Protorhinolophus shanghuangensis	Shanghuang fissure B	IVPP V18645.4	Left m_3	1.6	1.04		
Protorhinolophus shanghuangensis	Shanghuang fissure A	IVPP V18644.17	Right C^1	1.79	1.04	2.74	Figs 3A and 4A
Protorhinolophus shanghuangensis	Shanghuang fissure A	IVPP V18644.18	Rihgt C1	1.84	1.18	2.64	
Protorhinolophus shanghuangensis	Shanghuang fissure A	IVPP V18644.19	Right C^1	1.79	1.12	2.36	
Protorhinolophus shanghuangensis	Shanghuang fissure A	IVPP V18644.20	Right C^1	1.8	0.98	2	
Protorhinolophus shanghuangensis	Shanghuang fissure C	IVPP V18648.2	Right C^1	1.76	1.11	2.44	
Protorhinolophus shanghuangensis	Shanghuang fissure E	IVPP V18646.5	Left C^1	1.87	1.17	2.47	
Protorhinolophus shanghuangensis	Shanghuang fissure C	IVPP V18648.3	Left C^1	1.52	1.11	1.9	
Protorhinolophus shanghuangensis	Shanghuang fissure D	IVPP V18647.4	Right P^4	2.15	1.58		
Protorhinolophus shanghuangensis	Shanghuang fissure A	IVPP V18644.21	Left P^4	1.49	1.59		Figs 3B and 4B
Protorhinolophus shanghuangensis	Shanghuang fissure A	IVPP V18644.22	Left P^4	1.38	1.6		
Protorhinolophus shanghuangensis	Shanghuang fissure A	IVPP V18644.25	Right M^1	1.7	1.89		
Protorhinolophus shanghuangensis	Shanghuang fissure A	IVPP V18644.26	Right M^1	1.77	2.01		

Appendix 1. Continued

Taxon	Fissure	Specimen	Tooth	L	w	H	Figures
Protorhinolophus shanghuangensis	Shanghuang fissure B	IVPP V18645.5	Right M^1	1.78	2.3		
Protorhinolophus shanghuangensis	Shanghuang fissure B	IVPP V18645.6	Right M^1	1.88	2.32		
Protorhinolophus shanghuangensis	Shanghuang fissure C	IVPP V18648.4	Right M^1	1.55	2.06		
Protorhinolophus shanghuangensis	Shanghuang fissure D	IVPP V18647.5	Right M^1	1.69	2.09		
Protorhinolophus shanghuangensis	Shanghuang fissure A	IVPP V18644.23	Left M^1	1.84	2.06		Figs 3C and 4G
Protorhinolophus shanghuangensis	Shanghuang fissure A	IVPP V18644.24	Left M^1	1.73	2.23		
Protorhinolophus shanghuangensis	Shanghuang fissure B	IVPP V18645.7	Left M^1	1.84	2.18		
Protorhinolophus shanghuangensis	Shanghuang fissure C	IVPP V18648.5	Left M^1	1.97	1.97		
Protorhinolophus shanghuangensis	Shanghuang fissure E	IVPP V18646.6	Left M^1	1.79	2.25		Fig. 4C
Protorhinolophus shanghuangensis	Shanghuang fissure A	IVPP V18644.27	Right M^2	1.73	2.23		Fig. 4H
Protorhinolophus shanghuangensis	Shanghuang fissure A	IVPP V18644.28	Right M^2	1.74	2.35		
Protorhinolophus shanghuangensis	Shanghuang fissure A	IVPP V18644.29	Right M^2	1.67	2.29		
Protorhinolophus shanghuangensis	Shanghuang fissure A	IVPP V18644.30	Right M^2	1.68	2.23		Fig. 4F
Protorhinolophus shanghuangensis	Shanghuang fissure B	IVPP V18645.9	Right M^2	1.82	2.39		
Protorhinolophus shanghuangensis	Shanghuang fissure D	IVPP V18647.6	Right M^2	1.71	2.23		
Protorhinolophus shanghuangensis	Shanghuang fissure D	IVPP V18647.7	Right M^2	1.67	2.21		
Protorhinolophus shanghuangensis	Shanghuang fissure A	IVPP V18644.31	Left M^2	1.67	2.09		Fig. 3D
Protorhinolophus shanghuangensis	Shanghuang fissure C	IVPP V18648.6	Left M^2	1.77	2.19		
Protorhinolophus shanghuangensis	Shanghuang fissure C	IVPP V18648.7	Left M^2	2.02	2.5		Fig. 4D
Protorhinolophus shanghuangensis	Shanghuang fissure B	IVPP V18645.8	Left M^2	2.09	2.35		
Protorhinolophus shanghuangensis	Shanghuang fissure A	IVPP V18644.33	Right M^3	0.81	1.72		
Protorhinolophus shanghuangensis	Shanghuang fissure A	IVPP V18644.34	Right M^3	0.9	1.83		
Protorhinolophus shanghuangensis	Shanghuang fissure A	IVPP V18644.32	Left M^3	0.9	1.99		Fig. 3I
Protorhinolophus shanghuangensis	Shanghuang fissure B	IVPP V18645.10	Left M^3	0.91	1.86		Figs 3E and 4E
?Rhinolophidae	Shanghuang fissure B	IVPP V18649.1	Right M^2	1.4	1.75		Fig. 5C
?Rhinolophidae	Shanghuang fissure B	IVPP V18649.2	Left M^2	1.46	1.79		Fig. 5D
?Rhinolophidae	Shanghuang fissure B	IVPP V18649.3	Left M^3	1.01	1.58		Fig. 5E
Rhinolophoidea indet.	Shanghuang fissure C	IVPP V18650	Left $M^{1/2}$	1.3	1.45		Fig. 5B
?Rhinopomatidae	Shanghuang fissure A	IVPP V18651	Left M^2	1.7	1.9		Fig. 5A
Microchiroptera indet.	Shanghuang fissure E	IVPP V18652	Dentary fragment	0.81	0.73		Fig. 5F

Length (L), width (W) and height (H) in mm. Measures were made with a measurescope Nikon 10, coupled with a digital counter CM-26.

Appendix 2: Selected dental and mandibular characters for the cladistic analysis

The selected characters and character states were established from direct observations and comparisons, or from the available literature. All characters are considered as equally weighted and unordered. The score of '?' and '–' are used if information is unavailable due to a lack of material and if the character does not apply to a particular taxon, respectively.

Dentary

1. Coronoid process.
0. high (approximately ×2 the height of the tooth row)
1. low

2. Apex of the coronoid process.
0. pointed
1. rounded

3. Lower premolars.
0. aligned with axis of lower molars
1. oblique with the axis of the lower molars

4. Horizontal ramus of moderate thickness.
0. gracile (shallower than the teeth are tall)
1. robust (deeper than the teeth are tall)

5. Angle of the coronoid process.
0. nearly perpendicular to the horizontal ramus
1. sloping distally

6. Number of lower incisors on each side of jaw.
0. three lower incisors on each side of jaw
1. two lower incisors on each side of jaw

Lower teeth

7. Lower incisor size.
0. i1-2 subequal
1. i2 conspicuously larger than i1

8. i1.
0. trilobed
1. bilobed

9. p2 reduction.
0. reduced
1. very reduced (less than half p_4 height)
2. not reduced (p2 equal or larger than p_4)

10. p3.
0. present
1. absent

11. Development of p3.
0. well developed (larger than P2)
1. very reduced (not highly functional)
2. minute

12. Number of roots of p3.
0. two
1. one

13. Distolingual tubercle on p_4.
0. present
1. absent

14. Mesiolingual tubercle on p_4.
0. present
1. absent

15. Mesial low plate on p_4.
0. present
1. absent

16. Talonid basin of p_4.
0. extensive distally
1. very reduced

17. Buccal edge of p_4.
0. inflected
1. not inflected

18. Triangle of the trigonid of m1.
0. opened lingually
1. compressed mesiodistally

19. Triangle of the trigonid of m2.
0. opened lingually
1. compressed mesiodistally

20. Distance between paraconid and metaconid on m1-2.
0. less than the distance between the metaconid and entoconid
1. equal or greater than the distance between the metaconid and entoconid

21. Distance between paraconid and metaconid on m3.
0. less than the distance between the metaconid and entoconid
1. equal or greater than the distance between the metaconid and entoconid

22. Width of the talonid of m1-2.
0. talonid equivalent to trigonid
1. talonid wider than the trigonid
2. talonid less wide than the trigonid

23. Short cristid connecting the hypoconulid to entoconid.
0. present
1. absent

24. Position of the hypoconulid.
0. hypoconulid in median position
1. hypoconulid conspicuously displaced distobuccally
2. hypoconulid nearby and distobuccal to the entoconid

25. Entocristid.
0. straight
1. curved

26. Width of the talonid of m3.
0. talonid equivalent than the trigonid
1. talonid less wide than the trigonid

Upper Teeth

27. Buccal cingulum of C1.
0. well marked
1. faint or absent

28. C1 distal accessory cusp.
0. absent
1. present

29. Tubercle of C1.
0. strongly canted distally
1. slightly canted distally

30. Position of P2.
0. centred in the tooth row
1. displaced buccally in the toothrow
2. displaced lingually

31. Crown of P4.
0. waisted mesiodistally
1. not waisted mesiodistally

32. Lingual bassin of P4.
0. reduced
1. lingually extensive

33. Mesiolingual tubercle on P4.
0. present
1. absent

34. Mesiobuccal lobe of P4.
0. present
1. absent

35. Postparacrista of P4.
0. faintly curved buccodistally
1. inclined buccodistally

36. Crown of M1-2.
0. waisted mesiodistally
1. not waisted mesiodistally

37. Ectoflexus on M1-2.
0. simple
1. double

38. Buccal cingulum on M1-2.
0. surrounded paracone
1. surrounded both paracone and metacone
2. continuous all along the lingual edge
3. absent

39. Mesiobuccal notch between the parastyle and precingulum on M1-2.
0. deep
1. faint or absent

40. Centrocristae.
0. well-developed
1. shorter than lateral cristae (i.e. preparacrista and postmetacrista)

41. Position of the mesostyle.
0. retracted to the buccal edge
1. projected buccally

42. Mesostyle.
0. well developed
1. strongly reduced

43. Paraloph on M1-2.
0. present
1. absent

44. Metaloph on M1-2.
0. present
1. absent

45. Protofossa.
0. extended buccally between paracone and metacone
1. not extended buccally

46. Faint hypocone.
0. present
1. absent

47. Extension of the postprotocrista on M1-2.
0. extends to the postcingulum
1. does not reach nor the postcingulum, neither the lingual cingulum

48. Extension of the preprotocrista.
0. extends to the precingulum
1. does not reach the precingulum

49. Precingulum.
0. large
1. thin
2. discontinuous

50. Postcingulum.
0. connected to the lingual cingulum
1. not connected to the lingual cingulum

51. Extension of the lingual cingulum.
0. continuous
1. discontinuous

52. Lingual cingulum.
0. thin
1. broad

53. Talon of the M1.
0. well-projected distolingually
1. moderately projected distolingually

54. Talon of the M2.
0. well-projected distolingually
1. moderately projected distolingually

55. Metacone on M3.
0. well-developed
1. strongly reduced
2. absent

56. Mesiobuccal notch between the parastyle and precingulum on M3.
0. deep
1. faint or absent

57. Premetacrista on M3.
0. present
1. absent

58. Lingual cingulum on M3.
0. present
1. absent

59. Buccal edge of M3.
0. straight
1. inflected

Appendix 3: Data matrix of the phylogenetic analysis

Taxa	1	2	3	4	5	6	7	8	9	10	11	12	13	14	15	16	17	18	19	20	21	22	23	24	25	26	27	28	29	30
Icaronycteris menui	?	?	0	1	?	0	?	?	0	0	0	0	0	0	1	0	1	1	1	0	1	0	0	0+1	0	0	0	0	1	0
Archaeonycteris brailloni	?	?	?	?	?	?	?	?	0	0	0	0	0	0	1	0	1	1	?	0	?	0	0	0+1	0	?	0	0	1	0
Palaeochiropteryx tupaiodon	0	0	0	1	0	0	0	0	1	0	0	0	0	0	1	0	0	1	1	0	0	1	0+1	1	0	0	0	0	1	1
Protorhinolophus shanghuangensis	1	1	1	0	1	1	?	?	0	0	1	1	0	1	0	0	0	0	1	1	0	0	0	1	0	1	1	0	1	?
Vaylatsia frequens	1	0	1	0	1	1	?	?	0	0	1	1	0	1	0	0	0	0	1	1	0	0	0	1	1	0	0	0	0	0
Rhinolophus ferrumequinum	1	1	0	0	1	1	0	0	1	0	2	1	1	1	1	0	0	0	1	1	0	0	1	2	1	0	0	0	1	1
Rhinolophus hipposideros	1	1	1	0	1	1	0	0	1	0	2	1	1	1	0	0	1	0	1	1	0	0	1	2	1	0	0	0	1	0
Palaeophyllophora oltina	0	0	0	1	0	1	?	?	0	0	2	1	0	1	0	0	0	0	0	1	1	2	0	0	0	1	0	0	0	?
Hipposideros lankadiva	0	0	0	0	1	1	1	0	1	1	–	–	1	1	1	1	1	0	1	1	1	0	1	2	0	1	1	0	0	1
Hipposideros speoris	1	0	0	0	0	1	1	0	0	1	–	–	1	1	0	1	1	0	1	1	1	0	1	2	1	1	1	1	0	1
Pseudorhinolophus schlosseri	0	?	1	0	0	1	?	?	0	1	–	–	1	1	1	0	1	0	1	1	1	0	1	2	0	0	1	0	0	0

Taxa	31	32	33	34	35	36	37	38	39	40	41	42	43	44	45	46	47	48	49	50	51	52	53	54	55	56	57	58	59
Icaronycteris menui	1	0	0+1	0	0	0	0	2	1	1	0	1	0	0	0	1	0	0	0	1	0	1	0	0	0	1	0	0	1
Archaeonycteris brailloni	0	0	0	0	0	0	0	2	1	1	0	1	0	0	0	1	0+1	0	0	1	0	1	0	0	?	?	?	?	?
Palaeochiropteryx tupaiodon	1	0	1	0	1	0	1	2	1	1	0	1	0	0	0	1	0	0	0	1	0	1	1	1	0	1	0	0	1
Protorhinolophus shanghuangensis	0	1	0	0	0	0	0	2	0+1	0	0	0	0+1	0+1	0	0+1	0	0	0	1	1	1	0	0	2	1	1	1	0
Vaylatsia frequens	0	1	0	0	0	0	1	1	0	0	1	0	0+1	0+1	0	0+1	0	0	1	1	1	1	0	1	0	0	0	0	1
Rhinolophus ferrumequinum	0	1	1	0	1	0	1	1	0	0	1	0	1	1	0	1	0	0	1	1	1	1	0	1	0	0	0	0	1
Rhinolophus hipposideros	0	1	0	0	0	0	1	0	0	0	1	0	1	1	0	1	0	0	1	1	1	1	0	1	0	0	0	0	1
Palaeophyllophora oltina	0	0	1	1	0	0	0	2	1	1	0	1	1	1	1	1	1	1	1	1	0	1	0	0	2	1	1	1	0
Hipposideros lankadiva	1	0	0	1	1	1	1	1	0	0	1	0	1	1	0	1	1	0	1	0	0	1	1	1	2	0	1	1	1
Hipposideros speoris	1	1	0	0	1	0	1	0	0	0	1	0	0	1	0	1	1	0	1	0	0	1	0	1	1	0	0	1	1
Pseudorhinolophus schlosseri	1	0	1	1	1	0	1	3	1	0	1	0	1	1	0+1	1	1	0+1	0	1	0	1	0	1	2	1	0	1	0

